INF5490 RF MEMS

L6: RF MEMS svitsjer, II

Dagens forelesning

- Design av RF MEMS svitsjer
  - Elektromekanisk design, II
  - RF design
- Eks. på implementasjoner
  - Struktur
  - Ytelse
  - Fremstilling
- Alternative strukturer og aktiveringsmekanismer
- Noen utfordringer

Elektromekanisk design

- Stress →

- Dynamiske forhold
  - Demping
  - Innvirkning fra aktiveringsspenningen

Stress

- Stress bygges inn under fremstillingen
  - F.eks. pga temperatur-variasjoner
    - ”Residual stress”
- Aksialt **tensilt stress** (tøyende spenning)
  - Fjærkonstanten k_z øker (strengen spennes)
  - k_z kan øke 20x når tensilt stress 0 → 300 MPa
  - Vpi kan øke 4.5x når tensilt stress 0 → 300 MPa
- Tensilt stress må inkluderes som designparameter!
  - Kan ikke elimineres, - må tas i betraktning
  - Tensilt stress **evalueres** ved å måle ”misalignment” av teststrukturer (forskyvning av mønstre) →

Micro strain gauge with mechanical amplifier

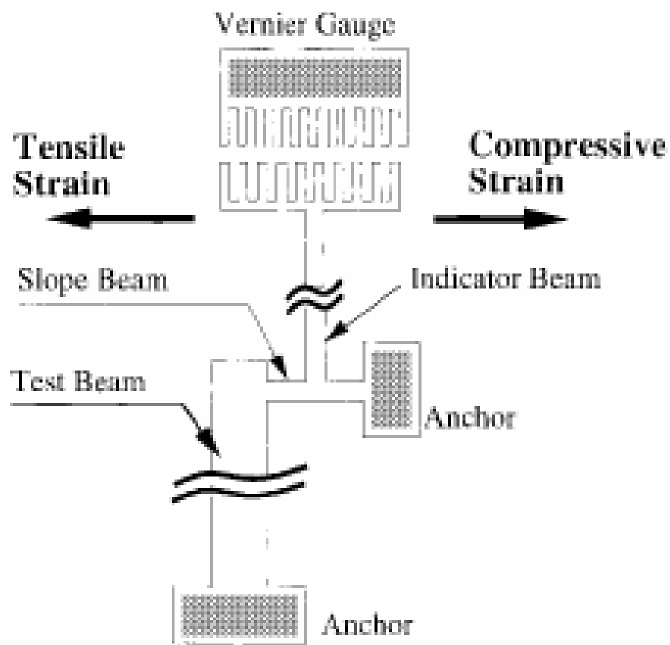

Fig. 1. Schematic diagram of a strain gauge based on the mechanical amplifier.

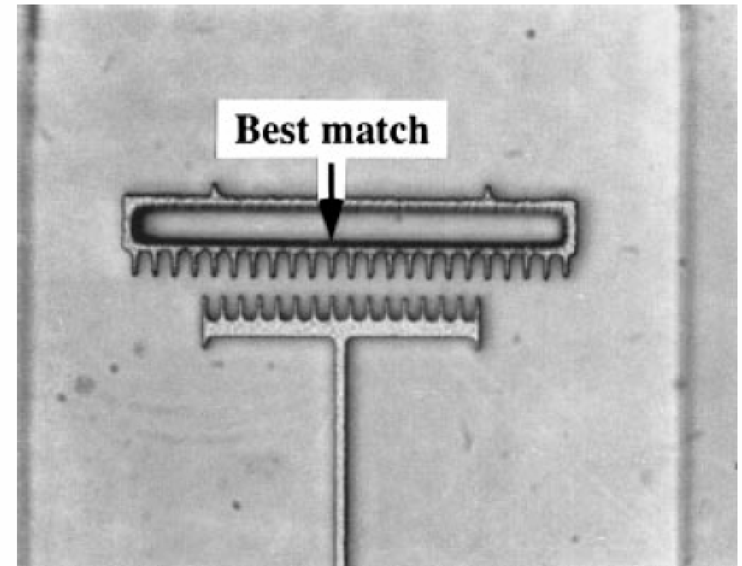

Fig. 4. An example of strain-gauge reading under an optical microscope.

Lin et al, J of MEMS, 1997

Svitsjehastighet og demping

- Svitsjehastighetn er avhengig av **demping**
  - Luft, gass må skyves vekk
  - **”squeezed-film damping”**
  - Modellering fra væske-mekanikk
- Hvordan redusere demping?
  - Operere i vakuum
    - Hermetisk kapslede pakker
  - Lage hull i membran
    - Perforert membran

Perforert membran

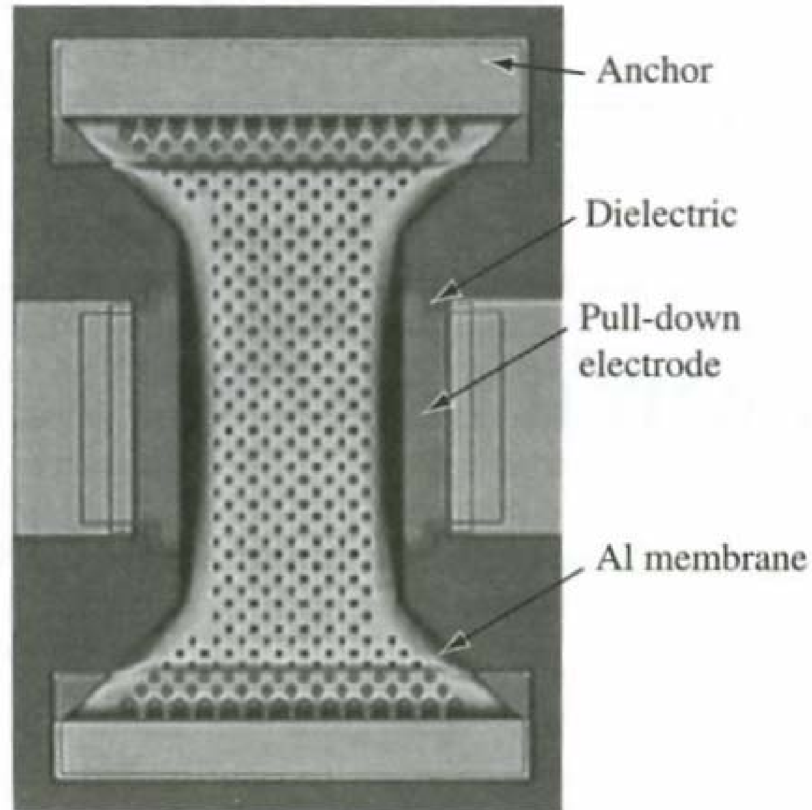

Figure 5.1. Photomicrograph of Raytheon MEMS capacitive shunt switch [2, 3] (Copyright IEEE).

Svitsjetider for Raytheon/TI-svitsjen

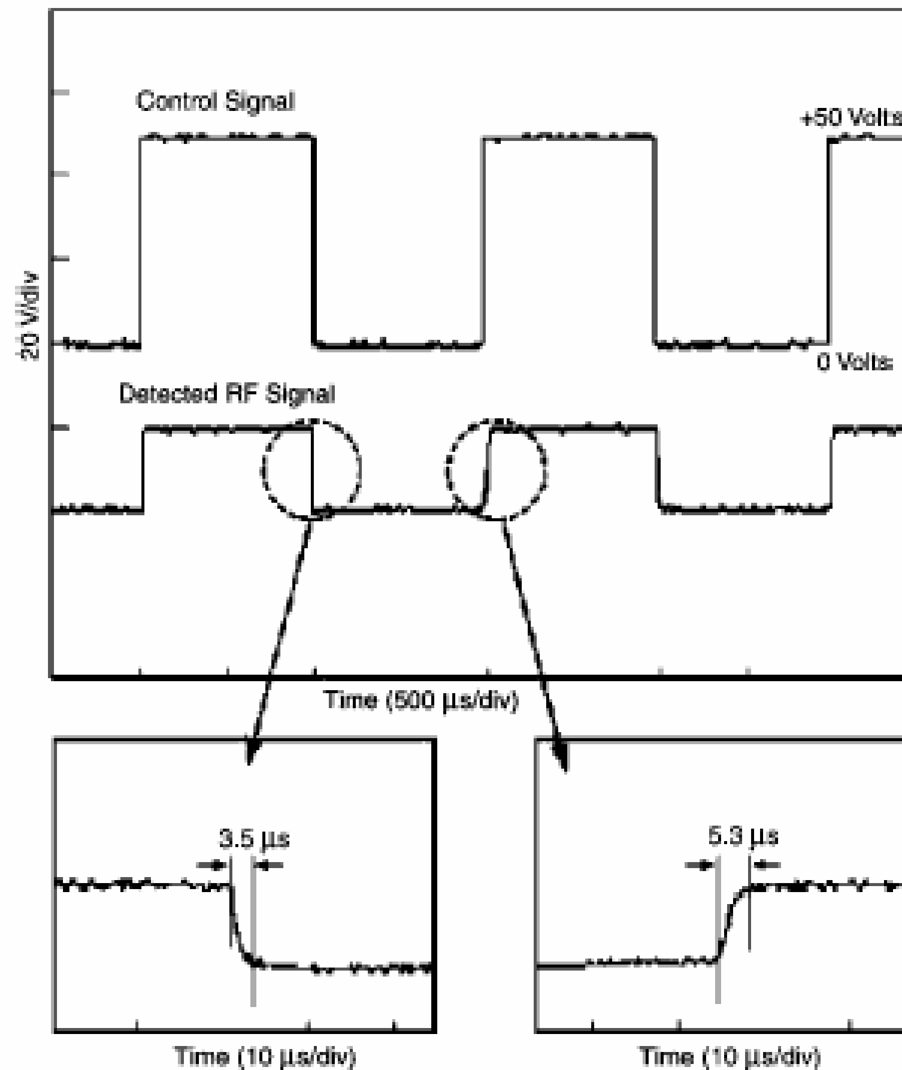

Figure 12. Switching time of the TI capacitive coupling shunt switch is of the order of 3.5–5.3 μs (from [30], Raytheon/TI).

Yao, 2000

Eks. på effekt av perforering

- → Betydelig hastighetsøkning ved perforert membran!

	No holes	With holes
b	1.3×10^{-3} Pa.s	2.1×10^{-6} Pa.s
τ_{sdown}	80μS	10.5μs

S. Pacheco, L.Katehi, Chapter in 'RF Technologies for Low Power Wireless Communications', Wiley, 2001.

Z..

Perforert membran: UMICH

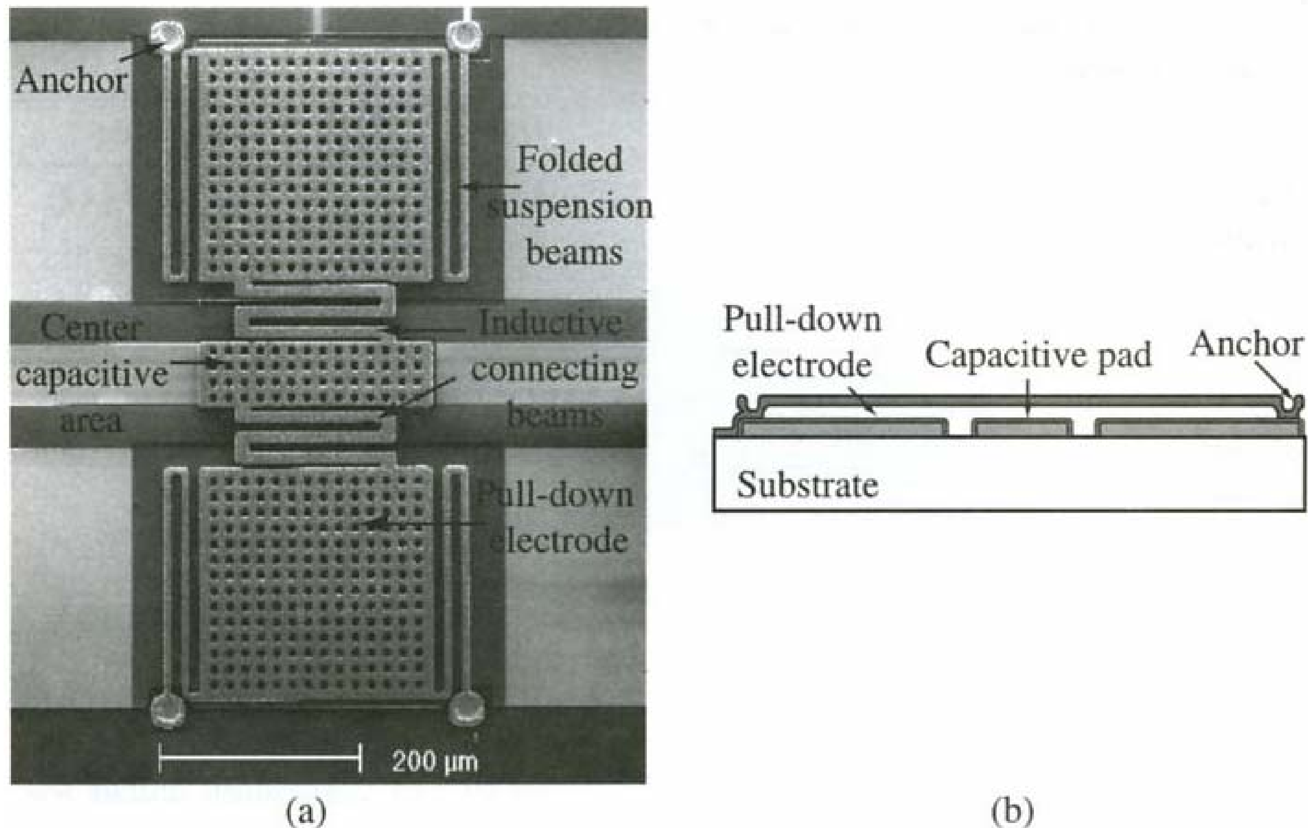

Figure 5.2. Photomicrograph of the university of Michigan low-voltage MEMS shunt switch. The number of meanders can be varied from 1 to 8 [7] (Copyright IEEE).

Gass-demping

Dynamisk respons til cantilever beam

$$m \frac{d^2w}{dt^2} + b \frac{dw}{dt} + k \cdot w = F_{ext}$$

w = displacement
b = dempekoeffisienten

$$\frac{W(j\omega)}{F(j\omega)} = \frac{1}{k} \frac{1}{1-\left(\frac{\omega}{\omega_0}\right)^2 + j\omega/(Q\,\omega_0)}$$

$$\omega_0 = \sqrt{\frac{k}{m}} =$$ resonansfrekvens

$$Q = k/(\omega_0 b) =$$ kvalitetsfaktor

Gass-demping, forts.

- m er **effektiv masse**
- Den effektive massen er forskjellig fra total masse siden bare enden (eller den sentrale delen) av bjelken beveger seg
  - $m_{eff} \sim 0.35 - 0.45 * m_{total}$
  - m_{eff} er avhengig av
    - Topologi
    - Tykkelsen av bjelken
    - Fjærkonstanten
    - Størrelsen på pull-down elektroden

Gass-demping, forts.

- Dempingen avhenger av **viskositeten**
  - Viskositet er motstand gassen yter mot transport
- Et uttrykk for demping av rektangulær parallell plate:

$$b = \frac{3}{2\pi} \cdot \frac{\mu \cdot A^2}{g_0^3}$$

$A =$ arealet

$g_0 =$ gapet

$\mu =$ viskositet til gassen

Gass-demping, forts.

Gass-dempingen påvirker Q-faktor

$$Q = k/(\omega_0 b) \qquad \rho = \text{fetthet}$$

$$Q_{cantilever} = \frac{\sqrt{E\rho}\, H^2}{\mu (WL)^2} g_0^3$$

$$Q_{cc} = \qquad \uparrow \; W \cdot L \rightarrow \frac{W \cdot L}{2}$$

for clamped-clamped beam

Rebeiz

Svitsje-hastighet

- Svitsje-hastigheten avhenger sterkt av Q-faktor og påtrykt spenning, Vs
  - Jo mindre demping, dess høyere Q-faktor
    - → økt svitsjehastighet
  - Systemet er **dempings-begrenset** ved $Q \leq 0.5$ [Castaner and Senturia]
  - Vs = konst * Vpi (pull-in) = (aktiverings-spenning)
  - Jo høyere spenning, dess sterkere elektrostatisk kraft
    - → økt svitsjehastighet

Tidsrespons for ulike Q-verdier

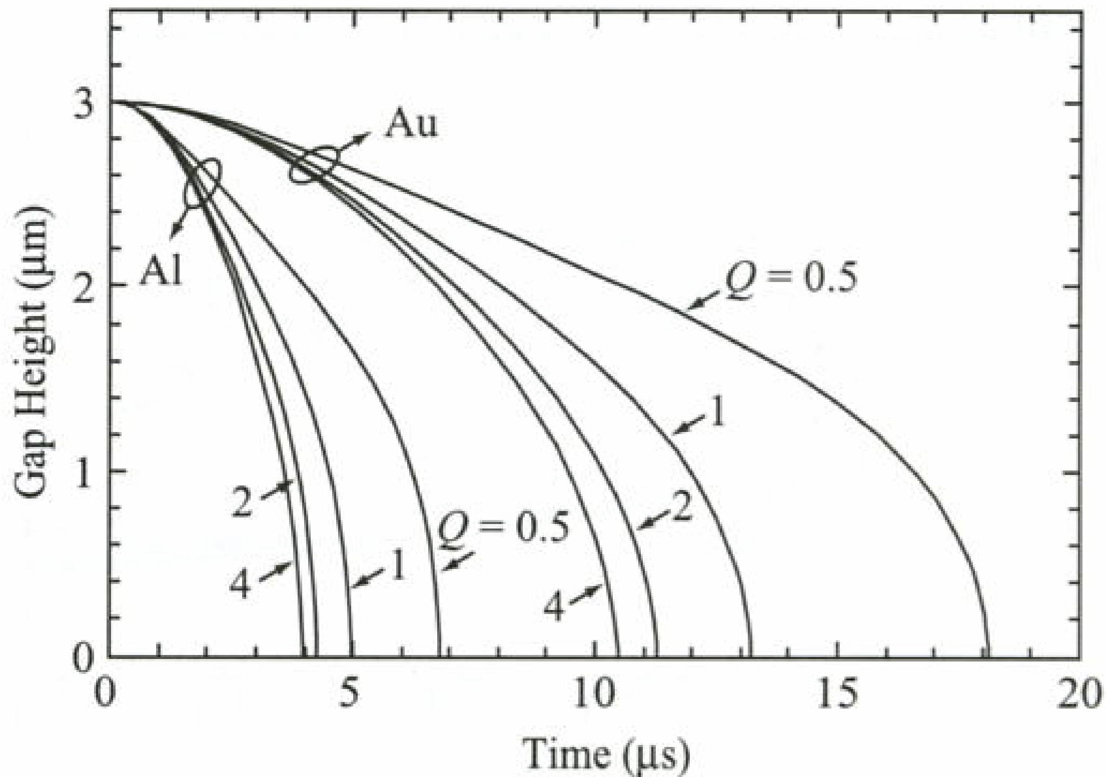

Figure 3.3. Pull-down simulations for the Au and Al beams of Table 3.1 for an applied voltage of 42 V ($V_s = 1.4V_p$).

Tidsrespons mhp. påtrykt spenning

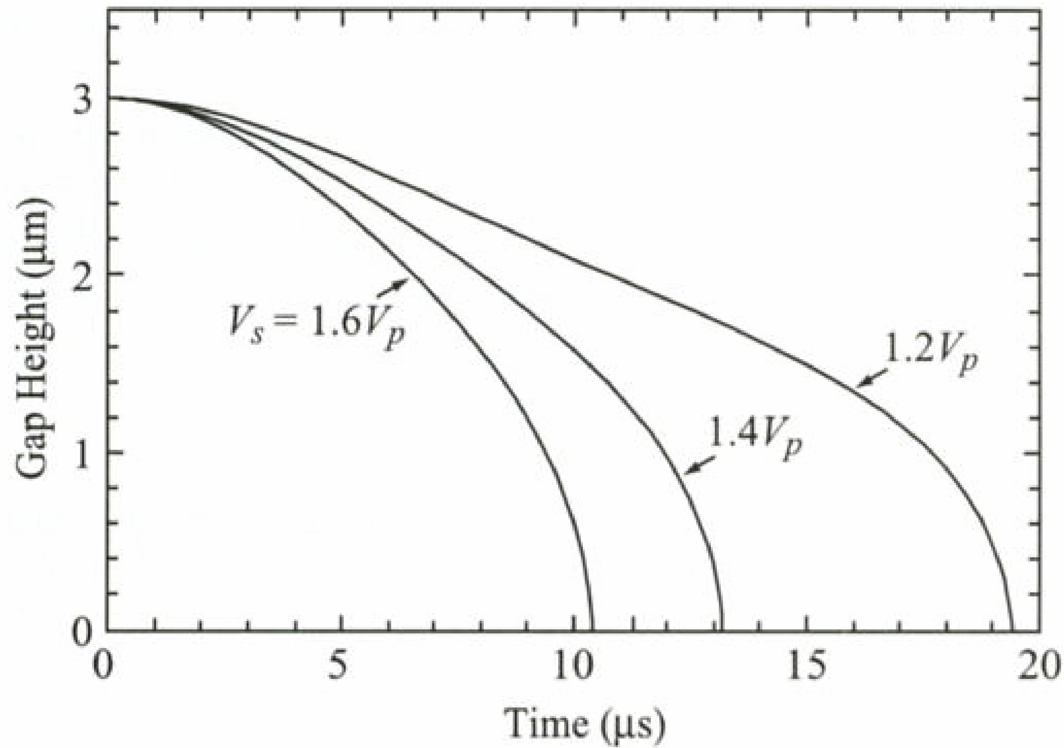

Figure 3.4. Pull-down simulations for the Au beam of Table 3.1 versus the applied voltage, and $Q = 1$.

Svitsje-hastighet, liten demping

Elektrostatisk kraft

$$F = \frac{\varepsilon_0 A V^2}{2 g^2}$$

Aksellerasjonsbegrenset svitsj (b~0)

$$m \frac{d^2 w}{dt^2} + k \cdot w = -\frac{\varepsilon_0 A V^2}{2 g_0^2} \quad (Q \geq 2)$$

Anvend spenning $V_s = \text{konst} \times V_{Pi}$

Svitsje-tid $t_s \approx 3.67 \frac{V_{Pi}}{V_s \cdot \omega_0}$

Rebeiz

Aksellerasjonsbegrenset svitsj

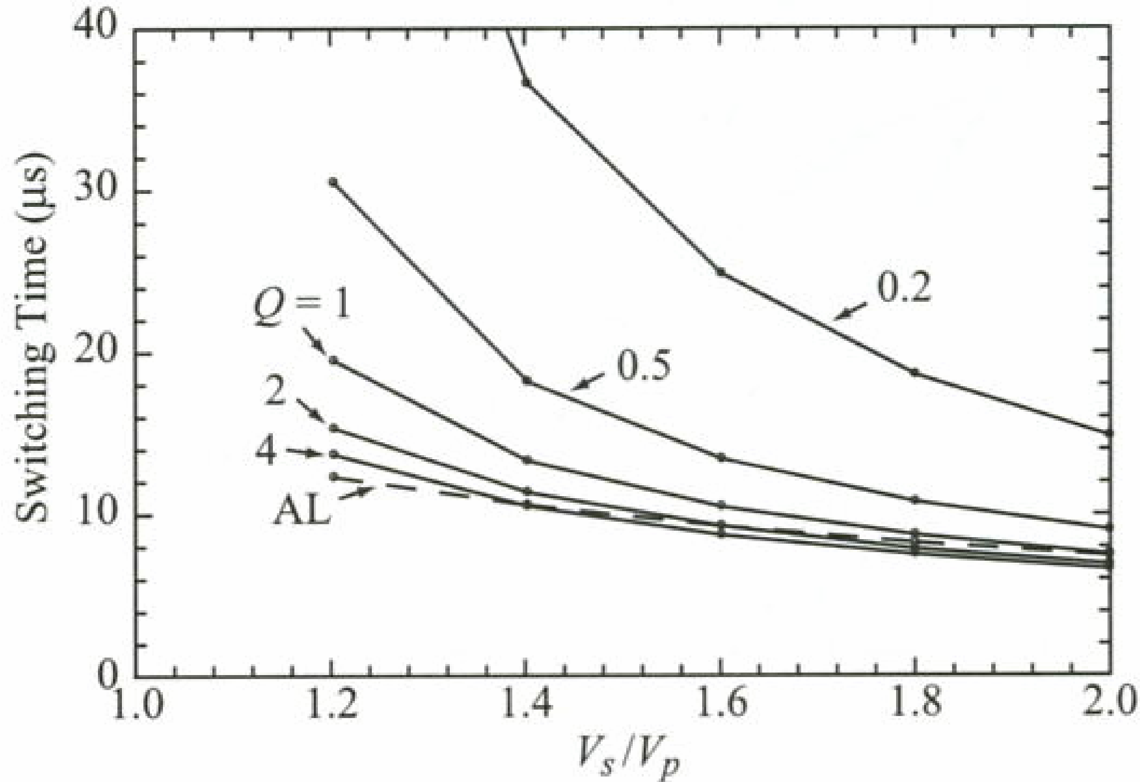

Figure 3.5. Simulated switching times for the Au beam given in Table 3.1. "AL" means acceleration-limited and is given by Eq. (3.23).

Svitsje-hastighet, stor demping

Ved et **dempings-begrenset** system

$$(Q \leq 0.5)$$

Bevegelsesligningen $$b \frac{dw}{dt} = F_{ext}$$

$$t_s \approx \frac{9 V_{Pi}^2}{4 \omega_0 Q V_s^2} \quad \text{for } V_s \gg V_{Pi}$$

Rebeiz

RF design

- Elektrisk modellering →
- S-parametre
- RF karakterisering
- Parasitter

RF design av MEMS svitsj

- Kan utføres ved full **elektromagnetisk** modellering
  - 3 dim elektromagnetisk analyse
    - Mekanisk modell, materialer, grensebetingelser
  - Beregning av felt-distribusjoner og S-parametre
- Bruk av ekvivalente krets-modeller →
  - Enkle modeller for håndkalkulering
    - Kan brukes til å beregne typiske RF ytelsesparametre

Ekvivalent-krets for kapasitiv svitsj

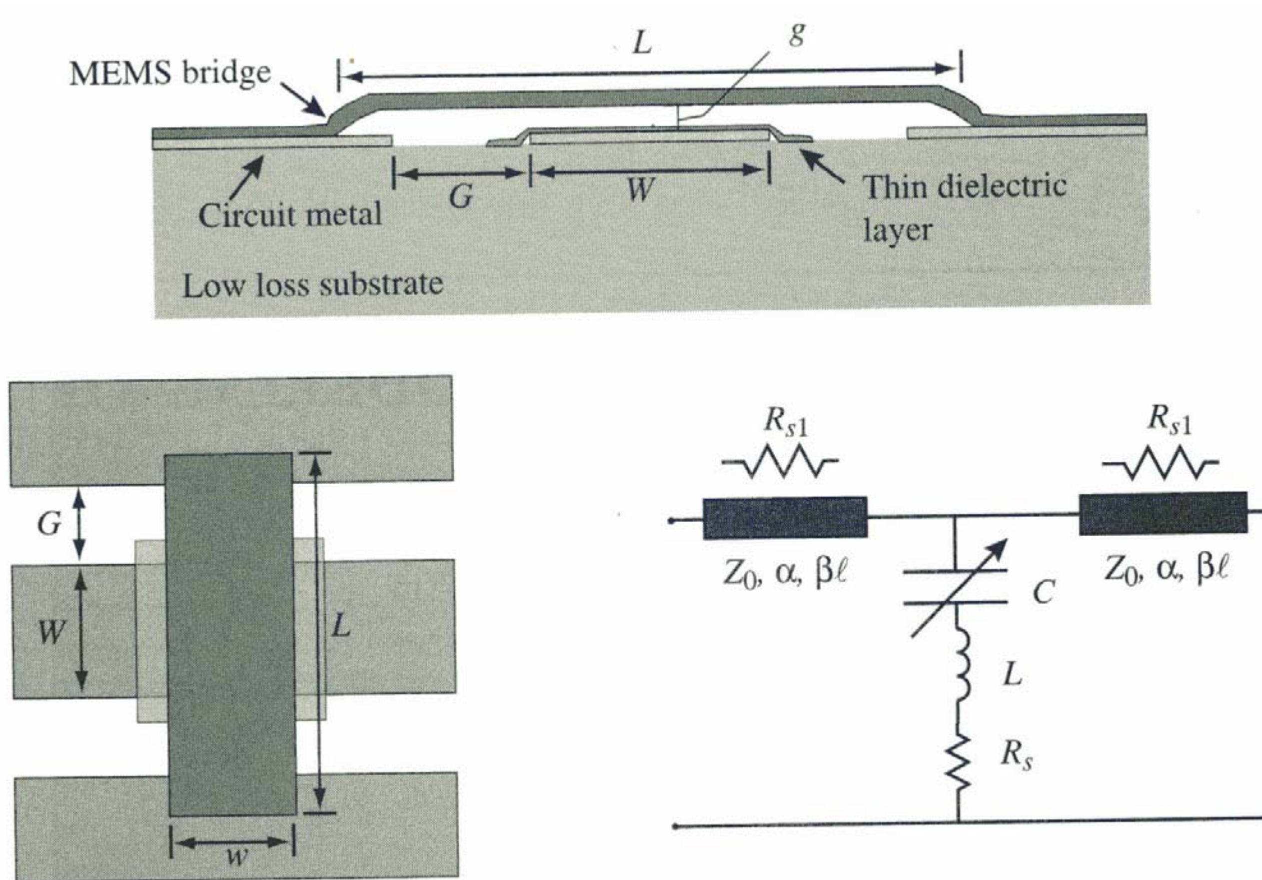

Figure 4.1. Illustration of a typical MEMS shunt switch shown in cross section and plan view. The equivalent circuit is also shown [6] (Copyright IEEE).

Rebeiz

Ekvivalent-krets, forts.

Svitsj shunt impedans

$$Z_s = R_s + j\omega L + \frac{1}{j\omega C}$$

$C = C_u$ eller C_d

Ved resonans

$$\omega_0 L = \frac{1}{\omega_0 C}$$

$$\omega_0 = \sqrt{\frac{1}{LC}}$$

$$Z_s = \begin{cases} \frac{1}{j\omega C} & \text{for } f \ll f_0 \\ R_s & \text{" } f = f_0 \\ j\omega L & \text{" } f \gg f_0 \end{cases}$$

Eksempel-verdier

Eks.

$C_u = 35\ fF \qquad C_d = 2.8\ pF$

$L = 7\ pH$

$f_0 = 322\ GHz$ up-state ← L liten betydning

$= 36\ GHz$ down-state

Forenklet beregning av ”transmission”

- Modell av kontakt seriesvitsj

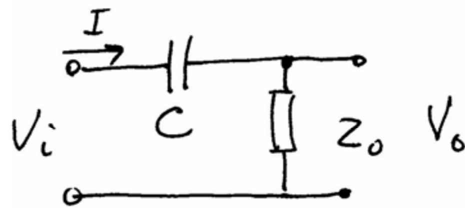

Serie svitsj i ”off”-tilstand

$$V_i = I \cdot \left(\frac{1}{sC} + Z_0 \right) \qquad V_o = I \cdot Z_0$$

$$\frac{V_o}{V_i} = \frac{Z_0}{Z_0 + \frac{1}{sC}} = \frac{sCZ_0}{1 + sCZ_0} \rightarrow \frac{j\omega C Z_0}{1 + j\omega C Z_0}$$

Transmisjon

$$\left| \frac{V_o}{V_i} \right|^2 = \frac{\omega^2 C^2 Z_0^2}{1 + \omega^2 C^2 Z_0^2} \begin{cases} \rightarrow 0 & \text{når } \omega \rightarrow 0 \\ \rightarrow 1 & \text{når } \omega \rightarrow \infty \end{cases}$$

Forenklet beregning av ”transmission”, forts.

- Modell av kontakt shunt svitsj

Shunt svitsj i ”off”-tilstand

$$I_i = \frac{V_0}{C \,//\, Z_0} \qquad I_0 = \frac{V_0}{Z_0}$$

$$\frac{I_0}{I_i} = \frac{V_0 / Z_0}{V_0 \Big/ \left(\dfrac{\frac{1}{sC} \cdot Z_0}{\frac{1}{sC} + Z_0} \right)} = \frac{1}{1 + sCZ_0}$$

$$\frac{I_0}{I_i} \rightarrow \frac{1}{1 + j\omega C Z_0}$$

Shunt svitsj, forts.

$$\frac{I_o}{I_i} \rightarrow \frac{1}{1 + j\omega C Z_0}$$

Transmisjon

$$\left| \frac{I_o}{I_i} \right|^2 = \frac{1}{1 + \omega^2 C^2 Z_0^2} \begin{cases} \rightarrow 1 \text{ når } \omega \rightarrow 0 \\ \rightarrow 0 \text{ når } \omega \rightarrow \infty \end{cases}$$

Sammenligning

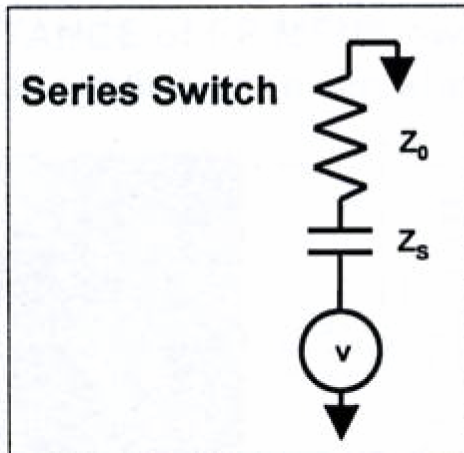

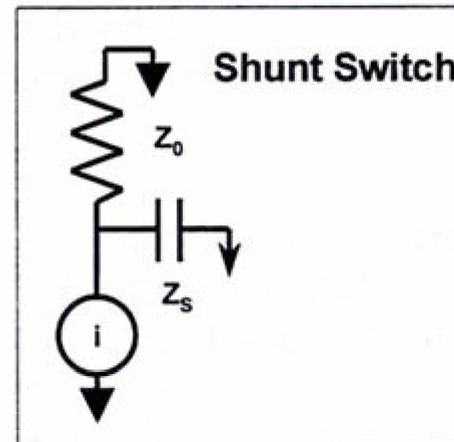

Transmission $\sim (\omega Z_0 C_S)^2 / [1 + (\omega Z_0 C_S)^2]$	Transmission $\sim 1 / [1 + (\omega Z_0 C_S)^2]$
$\rightarrow$ 0 as $\omega \rightarrow 0$	$\rightarrow$ 1 as $\omega \rightarrow 0$
$\rightarrow$ 1 as $\omega \rightarrow \infty$	$\rightarrow$ 0 as $\omega \rightarrow \infty$

Elektrisk karakterisering av RF MEMS svitsjer

- Ved lave frekvenser
  - Bruk impedans – admittans parametre
    - To-port med spenning og strøm
- Ved høye frekvenser
  - Bruk S-parametre
  - S-parametrene måles/beregnes når linjene er terminert med sin karakteristiske impedans
  - S-parametrene er småsignal-parametre: RF effekt < DC effekt

S-parametre

- 2-port for definisjon av S-parametre
- ”Power waves”

$$a_n = \frac{1}{2\sqrt{Z_0}}(V_n + Z_0 I_n) \quad (4.36a)$$

$$b_n = \frac{1}{2\sqrt{Z_0}}(V_n - Z_0 I_n) \quad (4.36b)$$

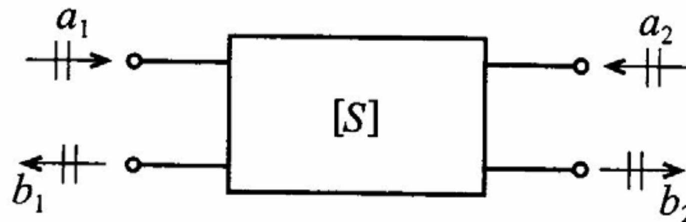

Figure 4-14 Convention used to define *S*-parameters for a two-port network.

Definisjon av S-parametrene

- Beregninger viser at effekten (power):

$$P_n = \tfrac{1}{2}\mathrm{Re}\{V_n I_n^*\} = \tfrac{1}{2}(|a_n|^2 - |b_n|^2)$$

S-parametre

$$\begin{Bmatrix} b_1 \\ b_2 \end{Bmatrix} = \begin{bmatrix} S_{11} & S_{12} \\ S_{21} & S_{22} \end{bmatrix} \begin{Bmatrix} a_1 \\ a_2 \end{Bmatrix} \qquad (4.41)$$

Hva hver enkelt parameter betyr

$$S_{11} = \left.\frac{b_1}{a_1}\right|_{a_2 = 0} \equiv \frac{\text{reflected power wave at port 1}}{\text{incident power wave at port 1}} \tag{4.42a}$$

$$S_{21} = \left.\frac{b_2}{a_1}\right|_{a_2 = 0} \equiv \frac{\text{transmitted power wave at port 2}}{\text{incident power wave at port 1}} \tag{4.42b}$$

$$S_{22} = \left.\frac{b_2}{a_2}\right|_{a_1 = 0} \equiv \frac{\text{reflected power wave at port 2}}{\text{incident power wave at port 2}} \tag{4.42c}$$

$$S_{12} = \left.\frac{b_1}{a_2}\right|_{a_1 = 0} \equiv \frac{\text{transmitted power wave at port 1}}{\text{incident power wave at port 2}} \tag{4.42d}$$

Måling av S-parametre

- S-parametrene måles når linjene er **terminert** med sin karakteristiske impedans

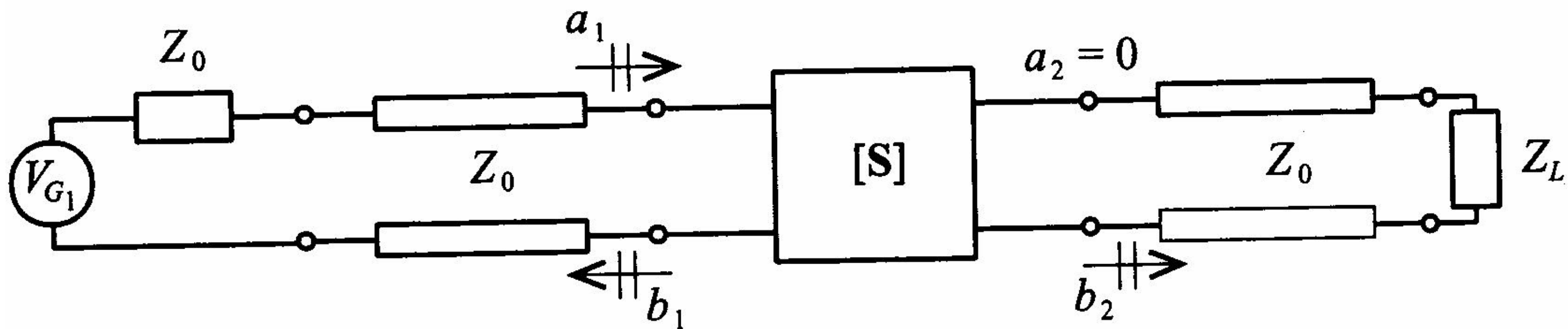

Figure 4-15 Measurement of S_{11} and S_{21} by matching the line impedance Z_0 at port 2 through a corresponding load impedance $Z_L = Z_0$.

RF karakterisering

- Reflekterte og transmitterte signaler må tas i betraktning
- Ulike parametre beregnes
  - Insertion loss i ON-state =
  - Isolation i OFF-state =
  - Return loss (begge tilstander) =

RF karakterisering, forts.

”Insertion loss” i ”on-state”

$$S_{21} = \left. \frac{b_2}{a_1} \right|_{a_2=0} = \frac{transmitted, port2}{incident, port1}$$

Spesifiseres i dB

Degraderes med økende frekvens

RF karakterisering, forts.

”Isolation” i ”off-state”

$$\frac{1}{S_{21}} = \left.\frac{a_1}{b_2}\right|_{a_2=0} = \frac{incident, port1}{transmitted, port2}$$

(Varadan)

$$\frac{1}{S_{12}} = \left.\frac{a_2}{b_1}\right|_{a_1=0} = \frac{incident, port2}{transmitted, port1}$$

(mest vanlig def)

→Stor isolasjon når utgang er liten i forhold til inngang
(eller når inngangen påvirkes lite av utgangen)

”Return loss” i begge tilstander

$$S_{11} = \frac{b_1}{a_1}$$

dvs. stort tap når mye reflekteres

Parameter-målinger

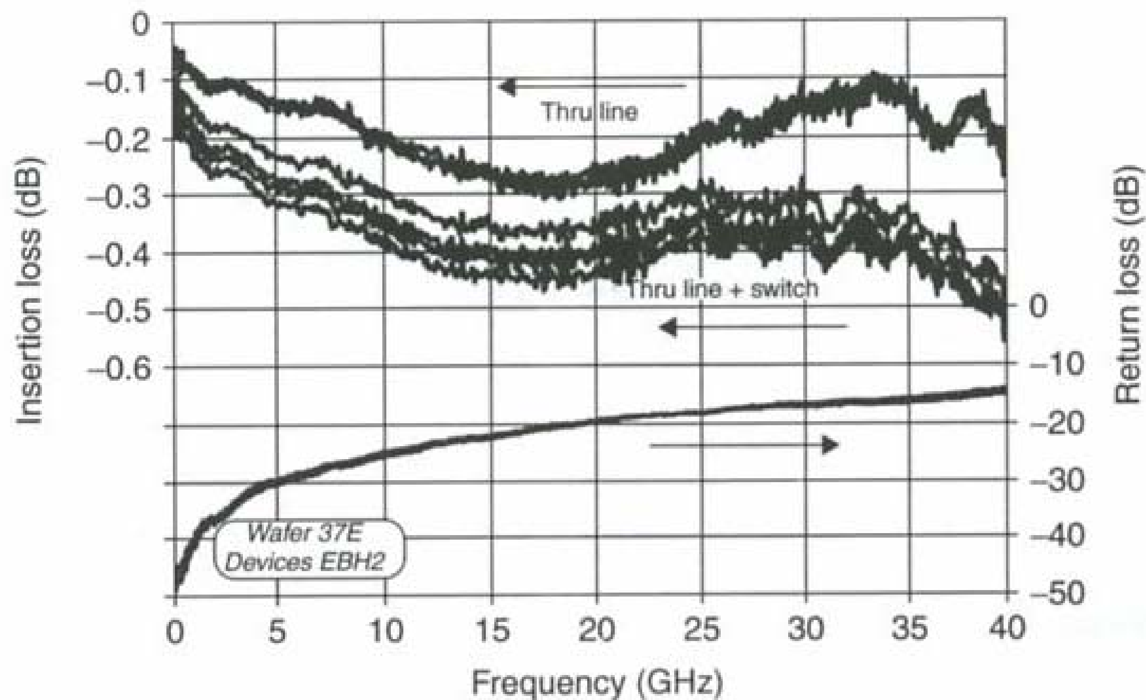

Figure 3.25 Measured insertion loss and return loss RF MEMS switch. Reproduced from C.L. Goldsmith, Z. Yao, S. Eshelman and D. Denniston, 1998, 'Performance of low-loss MEMS capacitive switches', *IEEE MW and Guided wave Letters* **8**(8): 269–271, by permission of IEEE, © 1998 IEEE

RF modellering

Shunt svitsj
Modelleres med kapasitans i ”up-state”

$$b_1 = S_{11} \cdot a_1 \Big|_{a_2 = 0}$$

Refleksjon $$\Gamma_0 = \frac{Z_L - Z_0}{Z_L + Z_0}$$

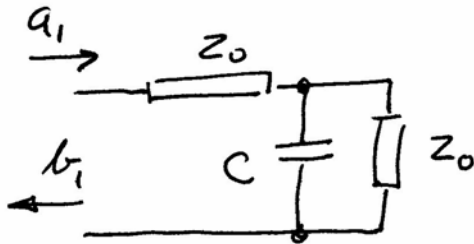

$$S_{11} = \Gamma_0 = \frac{C // Z_0 - Z_0}{C // Z_0 + Z_0} = \frac{\dfrac{\frac{1}{sC} \cdot Z_0}{\frac{1}{sC} + Z_0} - Z_0}{\dfrac{\frac{1}{sC} \cdot Z_0}{\frac{1}{sC} + Z_0} + Z_0}$$

RF modellering, forts.

$$S_{11} = \frac{-Z_0 s C}{2 + Z_0 s C}$$

$$S_{11} = \frac{-j\omega C_{up} Z_0}{2 + j\omega C_{up} \cdot Z_0}$$

For $\omega C_{up} Z_0 \ll 2$ $\quad |S_{11}|^2 = \dfrac{\omega^2 C_{up}^2 Z_0^2}{4}$

RF modellering, forts.

Shunt svitsj
Serie-resistans i "down-state" ved **resonans**

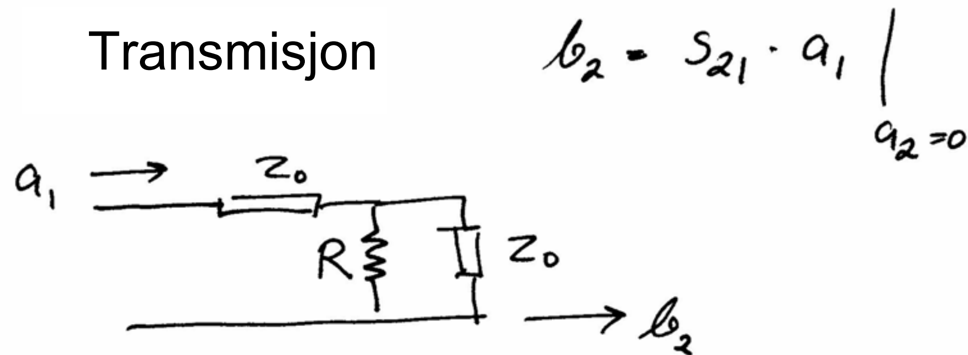

Transmittert effekt = 1 + reflektert

negativt

$$S_{21} = 1 + \frac{Z_L - Z_0}{Z_L + Z_0}$$

$$= \frac{2 Z_L}{Z_0 + Z_L} = \frac{2\, R // Z_0}{Z_0 + R // Z_0}$$

RF parasitter pga. meandere

- Meandere gjør fjæropphenget mykere
  - Flere ”grener” gir lavere Vpi
  - => fører til **parasitt induktans**
  - => påvirker RF-ytelsen

- Nøyaktig modellering må ta hensyn til parasitt induktans og parasitt resistans

Parasitt induktans

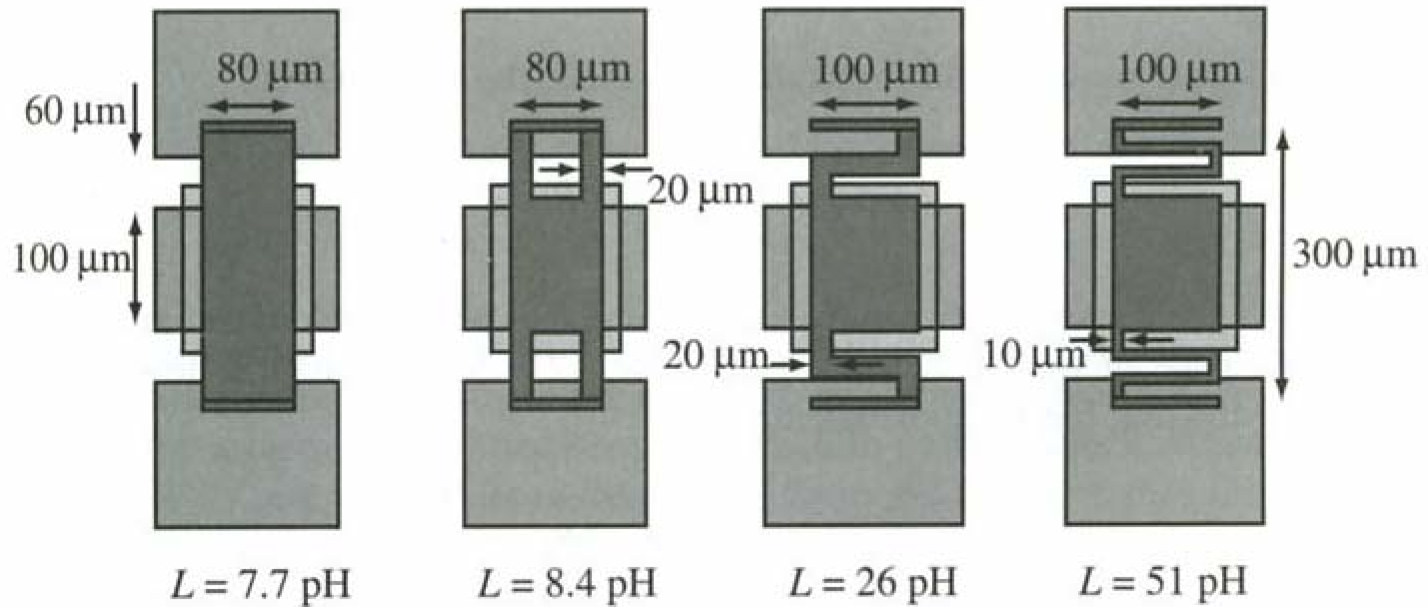

Figure 4.4. Simulated inductance for low-spring-constant MEMS bridges.

Rebeiz

Eksempler på implementasjoner

- Struktur og ytelse
  - **Serie-svitsjer**
    - Eks. på **kontakt-svitsjer** →
  - Shunt-svitsjer
- Fremstilling

Cantilever beam med elektrostatisk aktivering

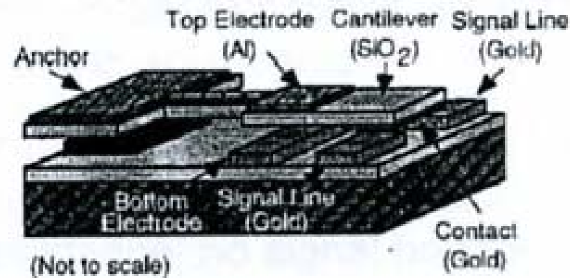

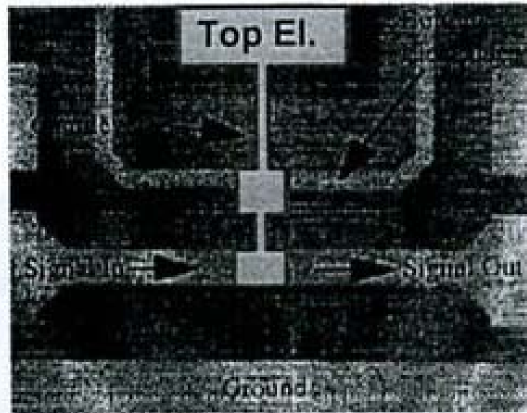

J.J. Yao, M.F. Chang, Solid-State Sensors and Actuators, 1995 and Eurosensors IX, Transducers '95.

Switch architecture:

- suspended SiO_2 cantilever arm
- **platinum-to-gold electrical contact**
- electrostatic actuation

Performance:

- **DC to RF range of frequency**
- **R_{DC}=0.22Ω**
- Pull in voltage=28V, max current=200mA
- speed: 30μs
- **-50dB isolation and 0.1dB insertion loss @ 4GHz**
- monolithic integration with IC because of the low temperature budget of the process

44

Rockwell serie-svitsj

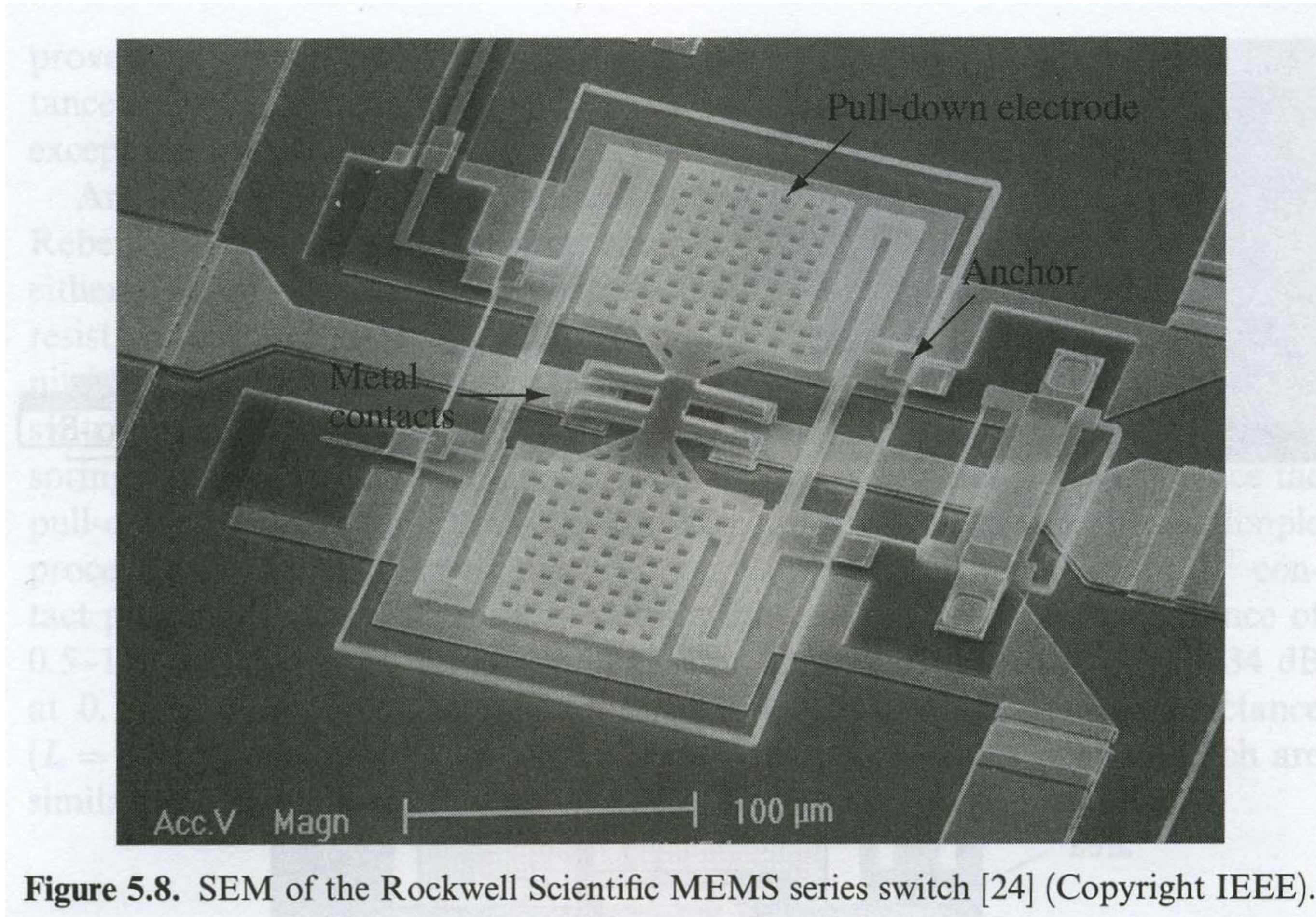

Figure 5.8. SEM of the Rockwell Scientific MEMS series switch [24] (Copyright IEEE).

Rockwell serie-svitsj, forts.

TABLE 5.6. Parameters for the Rockwell Scientific DC-Contact MEMS Series Switch

Parameter	Value	Parameter	Value
Length [μm]	250	Actuation area [μm^2]	75 × 75 (×2)
Width [μm]	150	Actuation voltage [V]	50–60
Height [μm]	2–2.5	Switch time [μs]	8–10
Cantilever type	Oxide, Au	Switch resistance [Ω]	0.8–2
Thickness [μm]	2, 0.25	C_u [fF]	1.75–2
Residual stress [MPa]	Low	Inductance [pH]	40–60
Spring constant [N/m]	15	Isolation [dB]	−50 (4 GHz)
Holes in cantilever	Yes	Isolation [dB]	−30 (40 GHz)
Sacrificial layer	Polyimide	Isolation [dB]	−20 (90 GHz)
Bridge release	Plasma etch	Loss [dB]	−0.1 (0.1–50 GHz)

Motorola

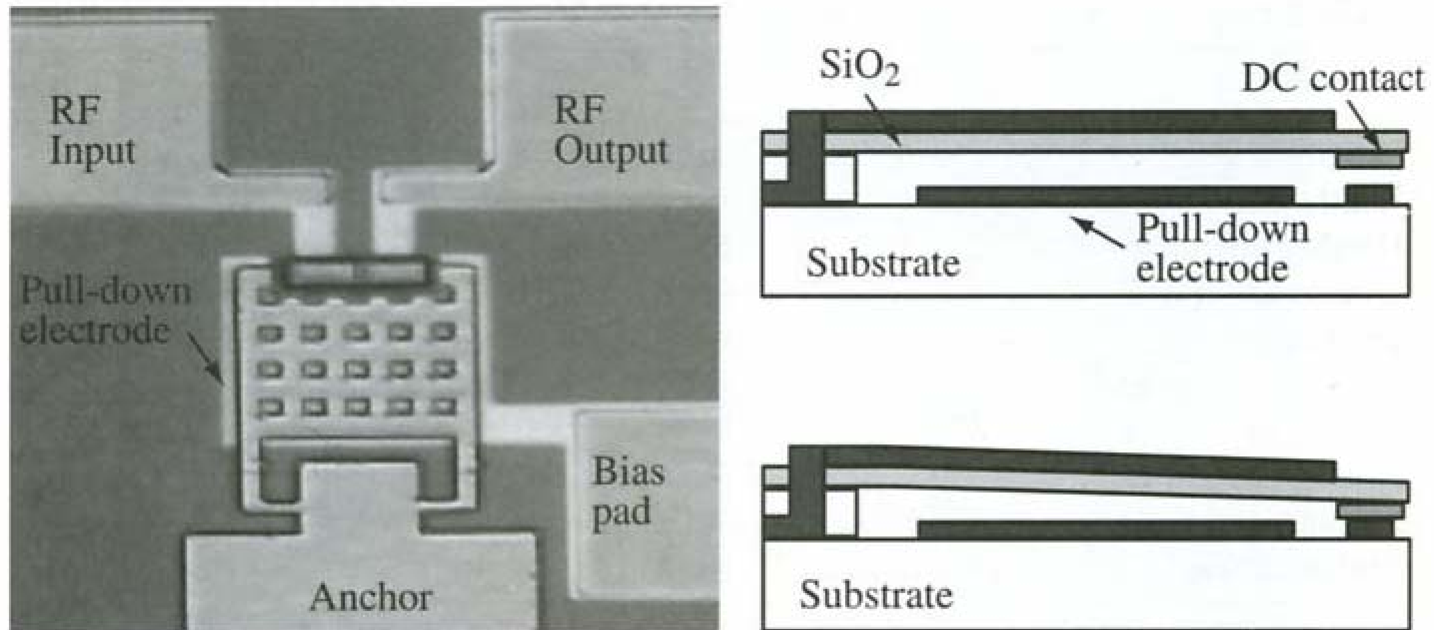

Figure 5.9. Photomicrograph of the Motorola DC-contact MEMS series switch and cross sections in the up- and down-state positions (Copyright IEEE).

Motorola, forts.

TABLE 5.7. Parameters for the Motorola DC-Contact MEMS Series Switch

Parameter	Value	Parameter	Value
Length [μm]	140	Actuation area [μm^2]	100×80
Width [μm]	100	Actuation voltage [V]	40–60
Height [μm]	2–3	Switch time [μs]	2–4
Cantilever type	Oxide, Au	Switch resistance, R_s [Ω]	1–2
Thickness [μm]	1.3, 0.3	C_u [fF]	2
Residual stress [MPa]	Low	Inductance [pH]	20
Spring constant [N/m]	35–40	Isolation [dB]	−44 (2–4 GHz)
Holes in cantilever	Yes (8 μm)	Loss [dB]	−0.15 (0.1–6 GHz)
Sacrificial layer	Polyimide		
Bridge release	Plasma etch		

Rebeiz

Lincoln

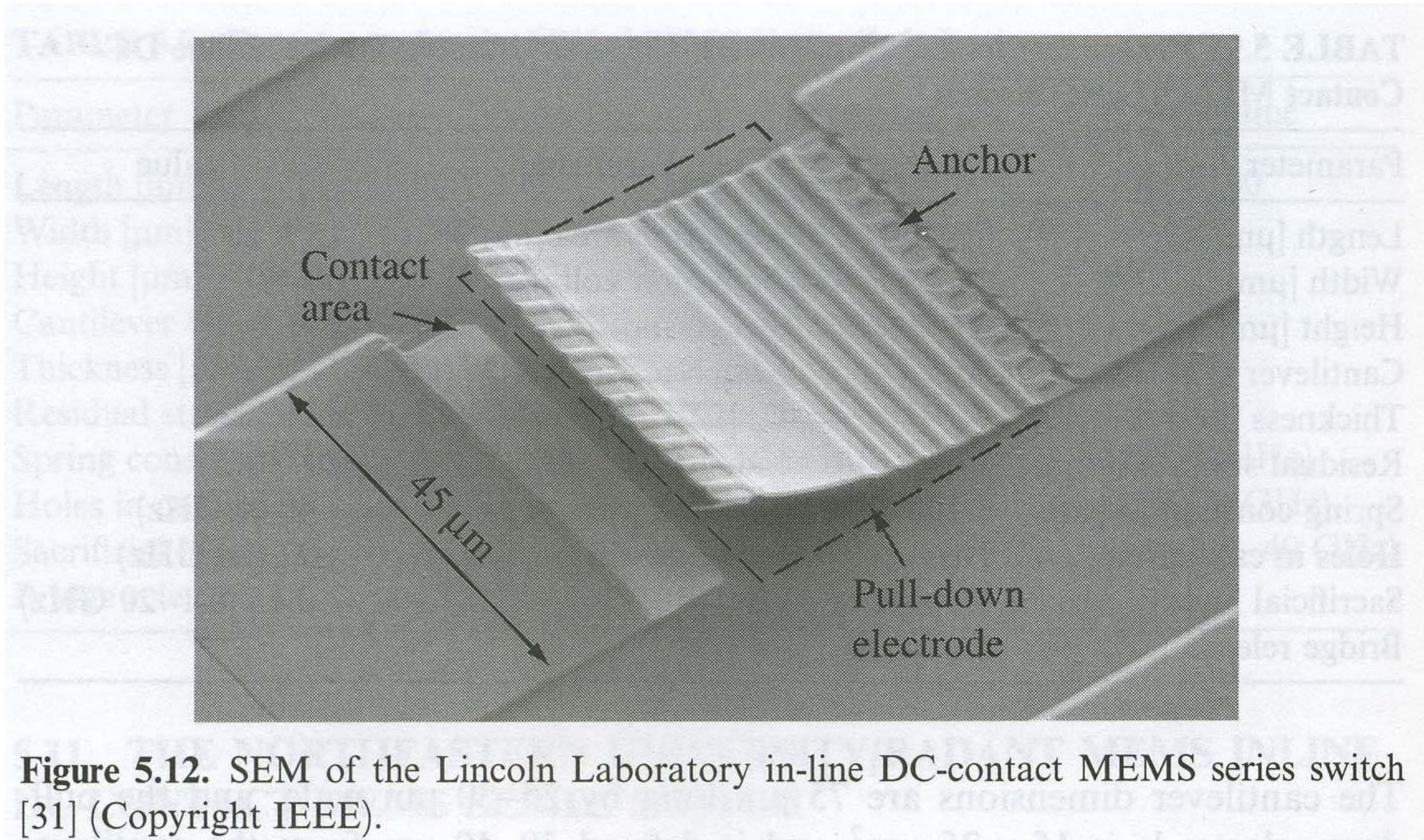

Figure 5.12. SEM of the Lincoln Laboratory in-line DC-contact MEMS series switch [31] (Copyright IEEE).

Lincoln, forts.

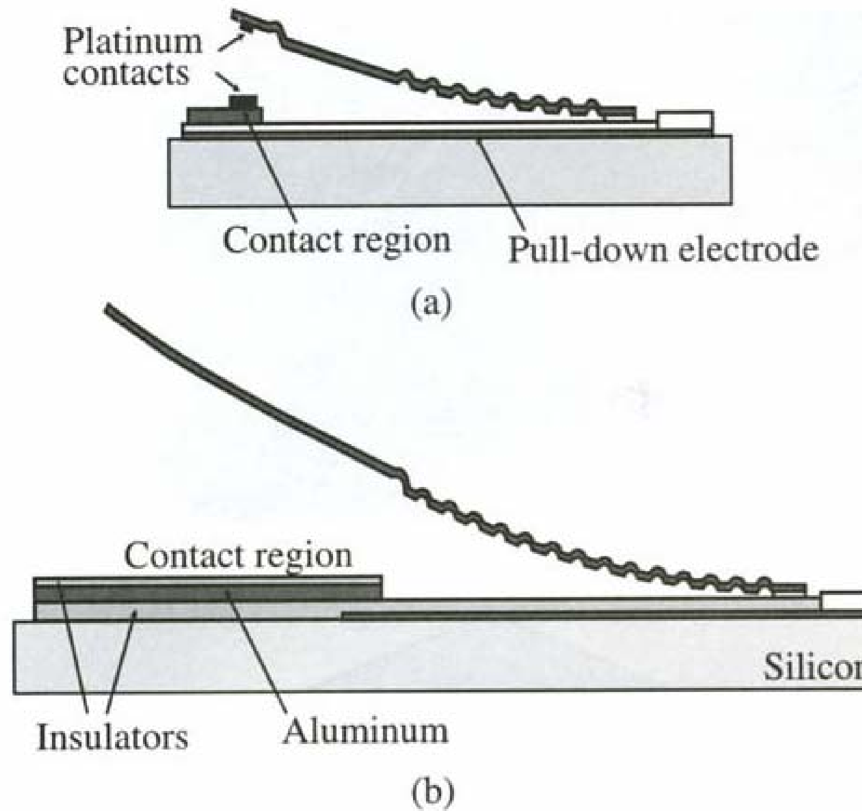

Figure 5.13. Cross section of the DC-contact (a) and capacitive-contact (b) Lincoln Laboratory inline switch (Copyright IEEE).

Lincoln, forts.

TABLE 5.10. Parameters for the Lincoln Laboratories Inline MEMS Series Switch

Parameter	Value	Parameter	Value
Length[a] [μm]	55/200	Actuation area [μm^2]	45 × 50
Width [μm]	50	Actuation voltage[b] [V]	30–80
Height [μm]	2–15	Switch time[b] [μs]	1–20
Cantilever type	Oxide, Al, oxide	Switch resistance, R_s [Ω]	1–2
Thickness [μm]	0.2, 0.5, 0.2	C_u [fF]	4–6
Residual stress	Very high	Inductance [pH]	Negligible
Holes in cantilever	No	Isolation [dB]	−40 (4 GHz)
Sacrificial layer	Polyimide	Isolation [dB]	−22 (30 GHz)
Bridge release	Freeze Drying	Loss [dB]	−0.15 (0.1–40 GHz)
Dielectric[c] (Å)	SiO_2 (1000)		

[a]Capacitive switch: 200 μm. DC-contact switch: 55 μm.
[b]Capacitive switch: 30–40 V and 20 μs; DC-contact switch: 60–80 V and <1 μs.
[c]Above pull-down electrode only.

Eks. på implementasjoner, forts.

- Shunt-svitsjer
  - **Kapasitive** RF MEMS svitsjer →

Kapasitive svitsjer, status

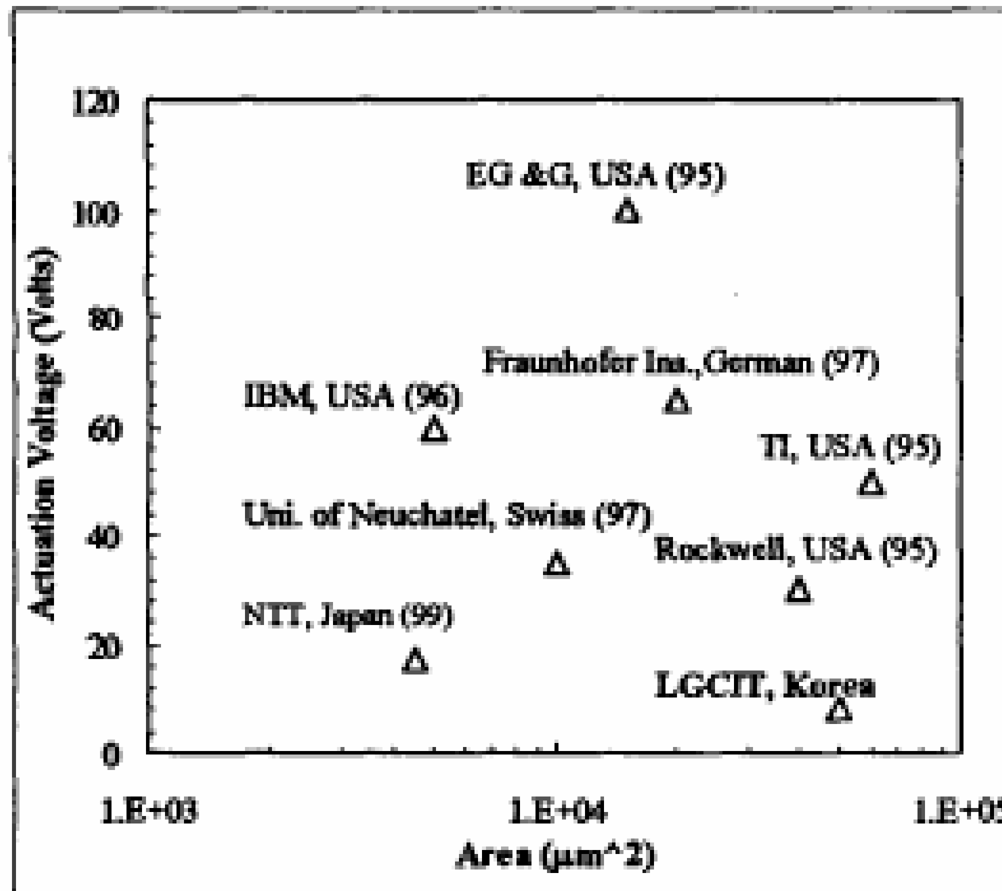

Figure 9. Comparison of actuation voltages of fabricated RF MEMS capacitive switches and previous mechanical capacitive switches [7]

Park et al 2000

Raytheon

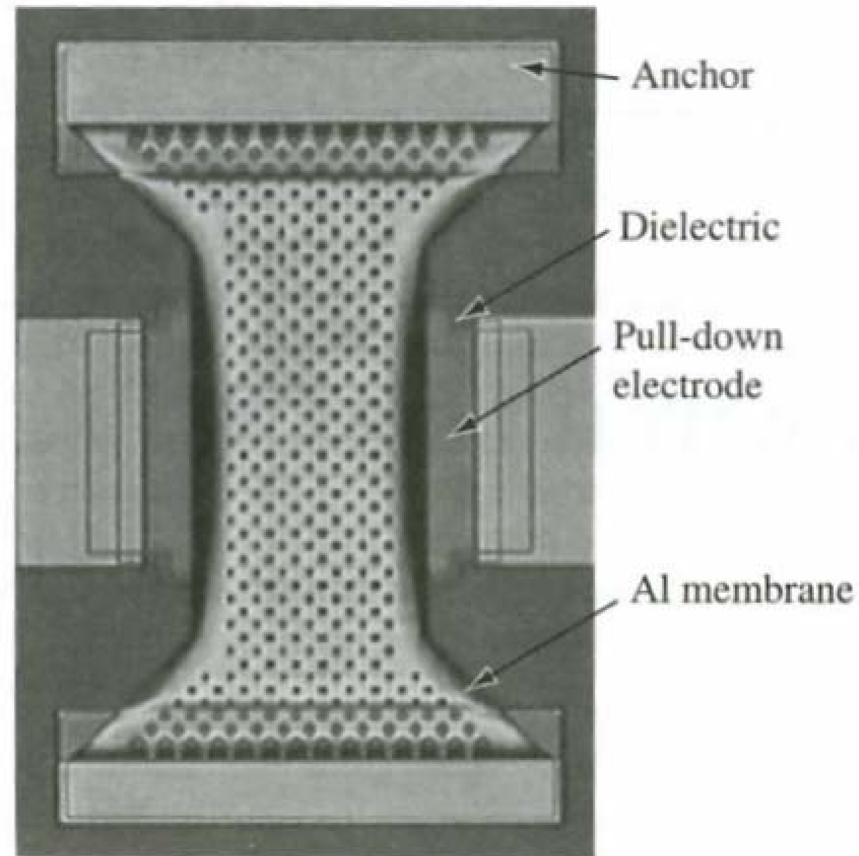

Figure 5.1. Photomicrograph of Raytheon MEMS capacitive shunt switch [2, 3] (Copyright IEEE).

Raytheon, forts.

TABLE 5.1. Parameters for the Raytheon Capacitive MEMS Shunt Switch

Parameter	Value	Parameter	Value
Length [μm]	270–350	Actuation area [μm^2]	80 × 100
Width [μm]	50–200	Actuation voltage [V]	30–50
Height [μm]	3–5	Switch time [μs]	3/5 (D/U)
Membrane type	Aluminum	C_d [pF]	1–6
Thickness [μm]	0.5	Capacitive ratio	80–120
Residual stress [MPa]	10–20	Inductance [pH]	5–10
Spring constant [Nm]	6–20	Resistance [Ω]	0.25–0.35
Holes [μm]	Yes (3–5)	Isolation [dB]	−20 (10 GHz)
Sacrificial layer	Polyimide	Isolation [dB]	−35 (30 GHz)
Bridge release	Plasma etch	Intermodulation	+66 dBm
Dielectric (Å)	Si_3N_4 (1000)	Loss [dB]	−0.07 (10–40 GHz)

Rebeiz

Univ of Michigan

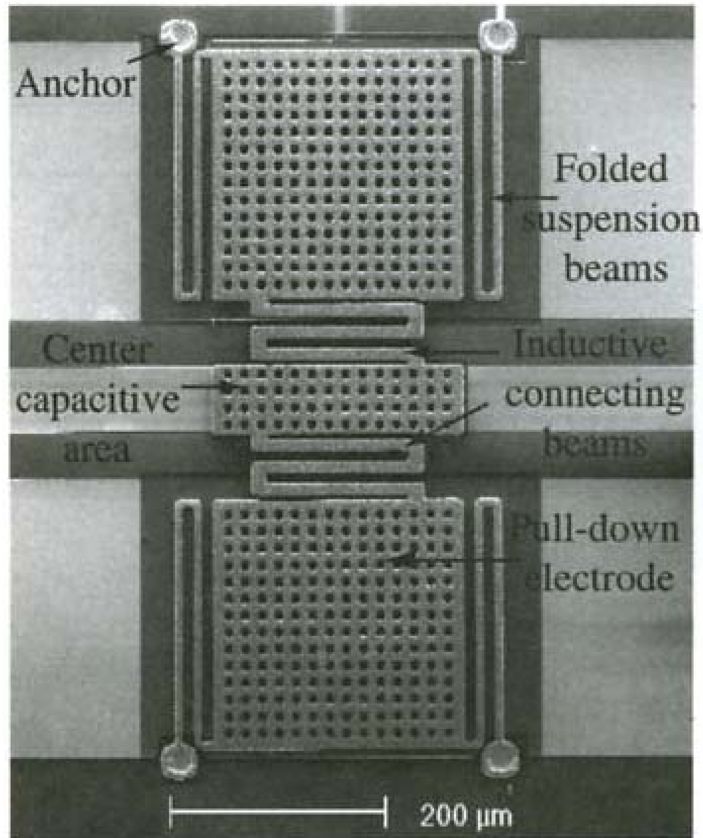

(a)

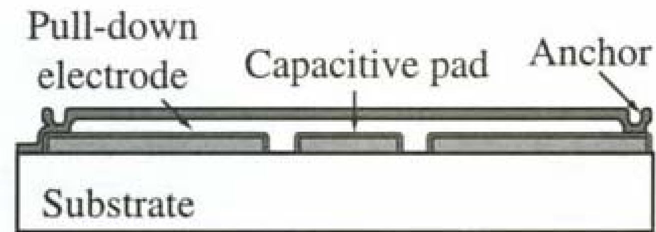

(b)

Figure 5.2. Photomicrograph of the university of Michigan low-voltage MEMS shunt switch. The number of meanders can be varied from 1 to 8 [7] (Copyright IEEE).

Univ of Michigan

TABLE 5.2. Parameters for the University of Michigan Low-Voltage MEMS Capacitive Shunt Switch

Parameter	Value	Parameter	Value
Length [μm]	500–700	Actuation area [μm^2]	200 × 200 (×2)
Width [μm]	200–250	Actuation voltage[a] [V]	6–20
Height [μm]	4–5	Switch time[a] [μs]	20–40 (D)
Membrane type	Nickel	C_d [pF]	1–3
Thickness [μm]	2–2.5	Capacitive ratio	30–50
Residual stress [MPa]	20–100	Inductance [pH]	1–2
Spring constant [N/m]	1–10	Resistance [Ω]	0.2–0.3
Holes [μm]	Yes (10)	Isolation [dB]	−25 (30 GHz)
Sacrificial layer	Polyimide	Intermodulation	N/A
Bridge release	Plasma etch	Loss [dB]	−0.1 (1–40 GHz)
Dielectric (Å)	Si_3N_4 (1000–1500)		

[a] Depends on number of meander support.

Rebeiz

Ulike ytelsesparametre

Table 1. Characteristics and performances of selected MEMS RF switches. Note, for the FET switch average GaAs MMIC FET switches are used for comparison.

Device characteristics and performance parameters	FET switch	Rockwell (RSC) [16, 26]	Raytheon/TI [28–30]	HRL Labs [19–20]	University of Michigan [27]
MEMS technology	—	Surface	Surface	Surface	Surface
Device size ($\mu m \times \mu m$)	$\sim$1 mm^2	80 × 160	120 × 280	$\sim$120 × 300	$\sim$1000 × 2000[a]
Current handling (mA)	$\sim$200	200	Not available	140	Not available
Structural material	GaAs	SiO_2	Al alloy	Si_xN_y	Plated Au
Actuation mechanism	—	Electrostatic	Electrostatic	Electrostatic	Electrostatic
Actuation voltage (V)	$\sim$1	$\sim$60	$\sim$50	$\sim$25	15–20
Contact mechanism	Semiconductor	Au based metal	Capacitive	Au	Capacitive
Insertion loss (dB)	2 at 6 GHz	0.2 (dc–40 GHz)	0.15 at 10 GHz 0.28 at 35 GHz	0.2 (dc–40 GHz)	0.6 (22–38 GHz)
Isolation (dB)	−22 at 2 GHz −20 at 6 GHz	−32 at 10 GHz −22 at 40 GHz	−15 at 10 GHz −35 at 35 GHz	−40 at 12 GHz −27 at 40 GHz	−40 at 22 GHz −50 at 35 GHz
Switching time	10 ns	2–5 μs	3.5–5.3 μs	20 μs	Not available
Lifetime (million cycles)	>100 000	$\sim$100 (cold) 10s (hot 1–40 mA)	500	$\sim$4 (hot 10 mA)	Not available
Others	Values may vary from device to device	third order IM product 71.5 dB below tone level	IP3 > +66 dBm	Unidentified resonance at 8.5 GHz	Tuned for 30 GHz performance

Yao, 2000

Ulike ytelsesparametre

Device characteristics and performance parameters	Northeastern University [21–23]	Siemens AG [24]	OMRON [31]	NEC Corporation [25]
MEMS technology	Surface	Bulk	Bonded wafer	Bonded wafer
Device size ($\mu m \times \mu m$)	Beam = 30×65	1.5 (mm^2)	2000×2500	250×900
Current handling (mA)	150	>100	Not available	Not available
Structural material	Au/Ni	Silicon epi	Silicon	P++ Silicon
Actuation mechanism	Electrostatic	Wedge electrostatic	Electrostatic	Electrostatic
Actuation voltage (V)	30–300	24	16–19	125
Contact mechanism	Au	Plated Au alloy	Au	Au
Insertion loss (dB)	Not available dc $R \sim 0.1$–$10\ \Omega$	Not available dc $R < 5\ \Omega$[b]	Not available dc $R \sim 0.5\ \Omega$	0.2 at 30 GHz
Isolation (dB)	Not available	Not available dc $R > 100\ G\Omega$	Not available	−13 at 30 GHz
Switching time	150 kHz cutoff	<0.2 ms	<0.3 ms	—
Lifetime (million cycles)	0.01–1000[c] (cold)	Not available (mechanical life 100)	1–10 (hot 10mA)	—
Others	500 million cycles for N_2 packaged hot-switch at 10 mA	Contact force is of the order of 1 mN	5 mN contact force Lifetime uses resistive load w/10 V	Double-hump design is used above

[a] Including four membrane switches to form a cross switch with short transmission lines.
[b] Including feed line resistance.
[c] Cold-switching lifetime depends on number of contacts ranging from 8 to 64.

Yao 2000

Fremstilling av kapasitiv svitsj

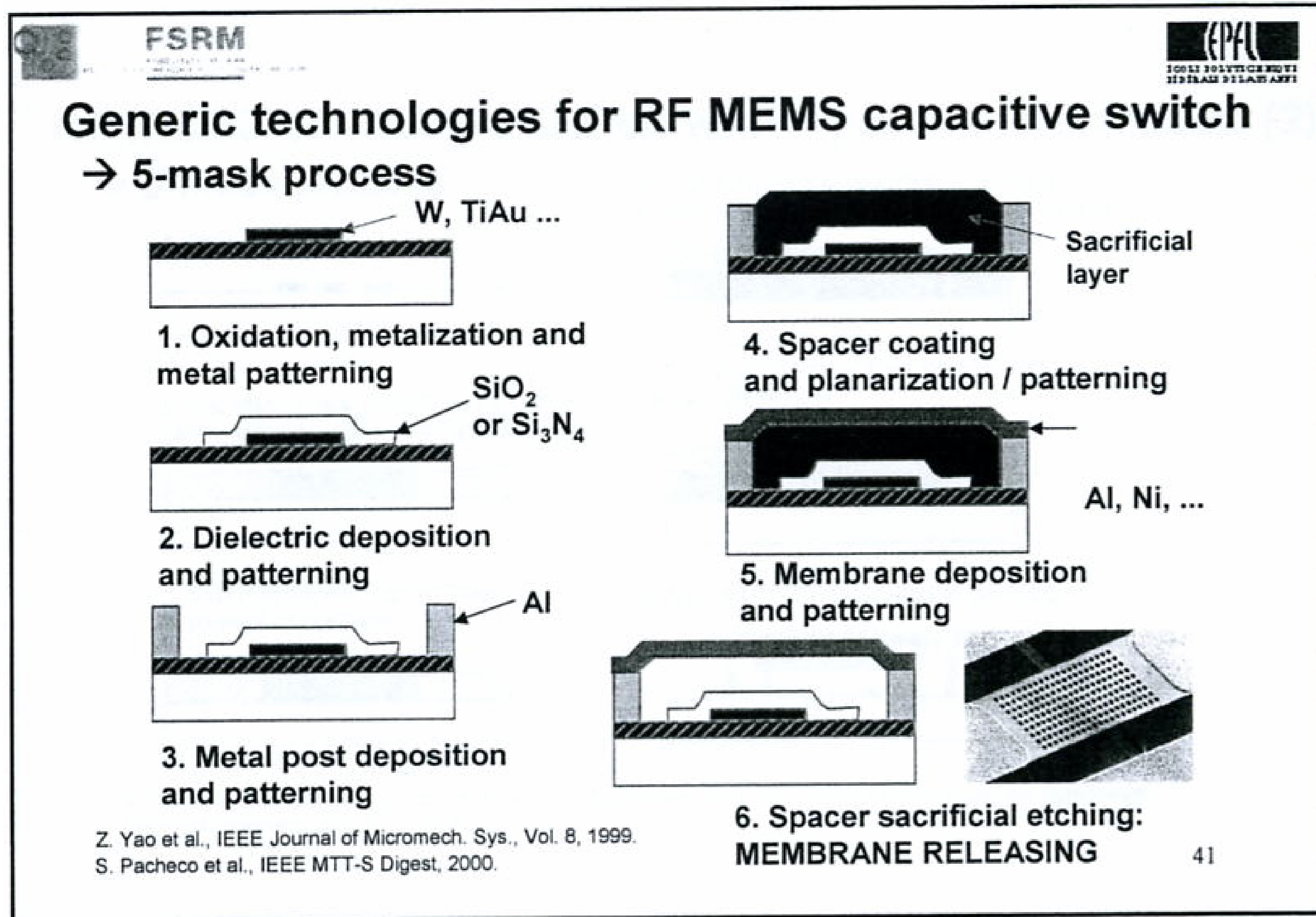

Fremstilling, ”Rockwell switch”

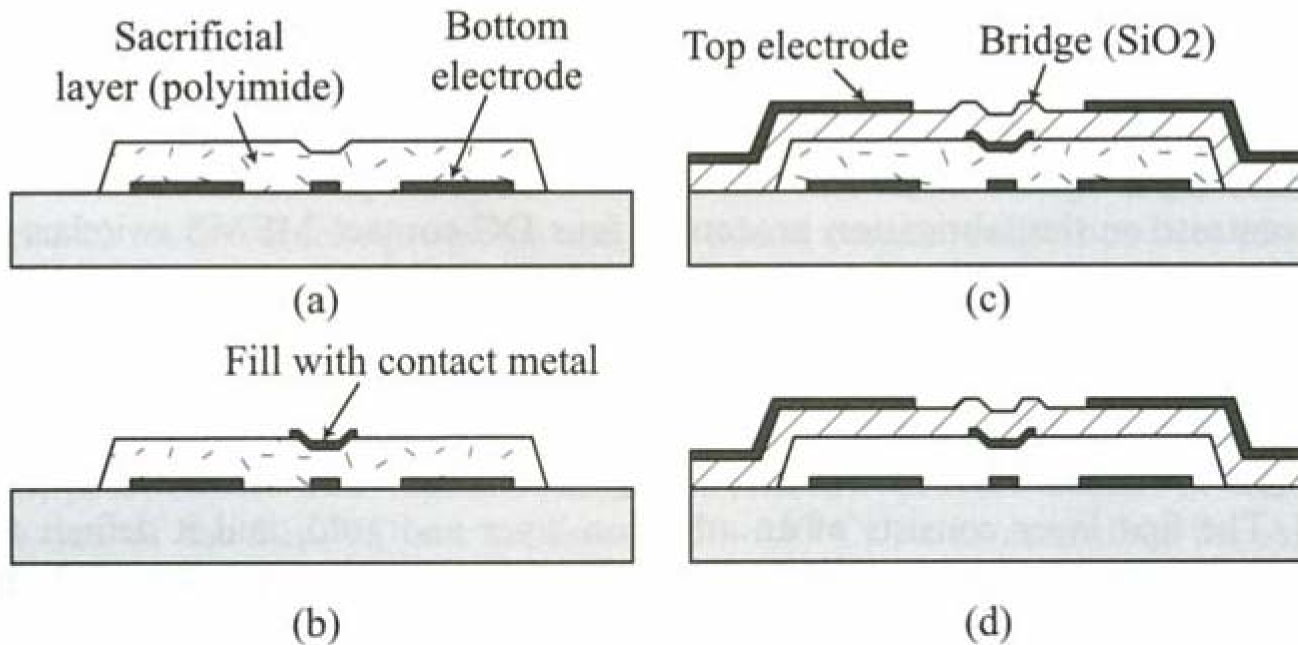

Figure 6.6. The fabrication process of the Rockwell Scientific series switch [8, 9].

Fremstilling, ”Michigan switch”

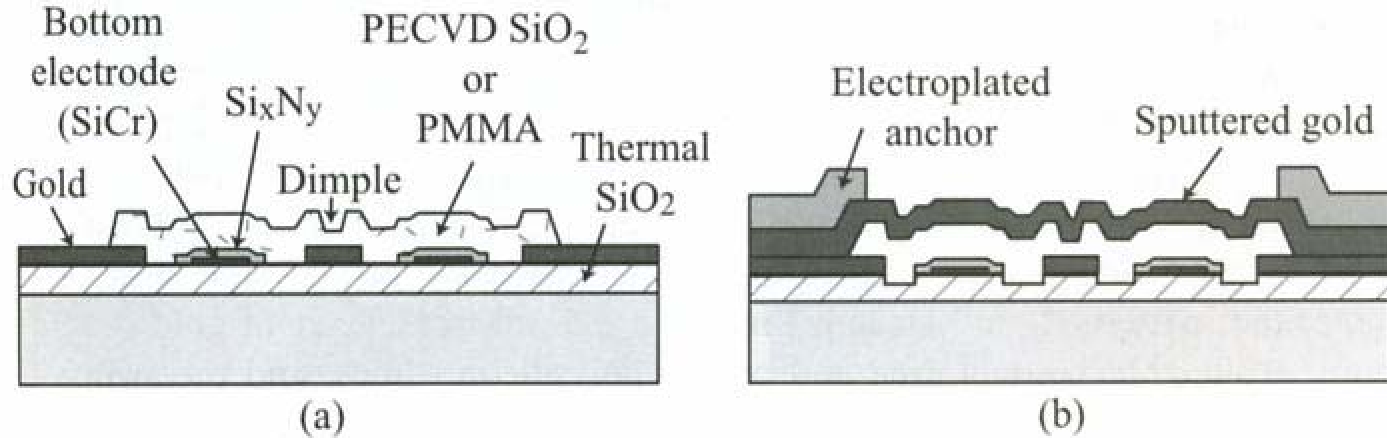

Figure 6.7. The fabrication process of the Michigan all-metal series switch [10, 11] (Copyright IEEE).

Rebeiz

Alternative svitsje-strukturer

- 3 elektroder kan også brukes
  - Topp-elektroden brukes for å ”clampe” den aktive elektroden til toppen
  - Spesielt viktig for systemer utsatt for høye aksellerasjoner

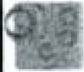

FSRM

RF MEMS capacitive switch with 3 parallel electrodes (1)

→Architecture with 3rd electrode: avoid switch movements in acceleration gradients (airborne systems, > 10g!)
→ 2nd bias used to clamp the 'active' electrode to the top

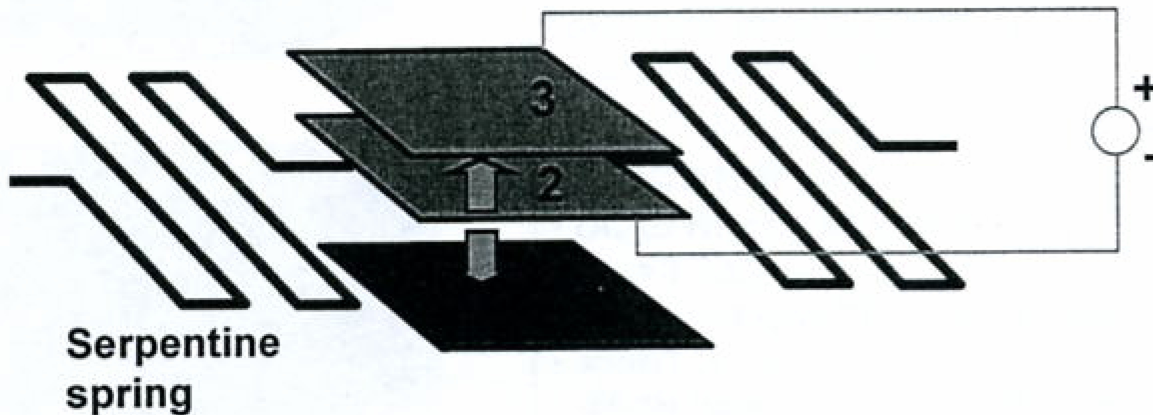

S. Pacheco, C. T.-C. Nguyen, and L. P. B. Katehi, Proceedings, IEEE MTT-S International Microwave Symposium, Baltimore, Maryland, June 7-12, 1998.

42

Alternative aktiveringsmekanismer

- Væske/metall kontakt-svitsj
  - Kan løse pålitelighetsproblemet en har pga. faststoff-til faststoff ved å bruke væske-til-faststoff
  - Kvikksølv (Hg) velges pga. dets egenskaper
    - Lav kontakt-resistans
    - Ingen signal-ringing
    - Ikke kontakt-slitasje
  - Elektrostatisk aktivering
    - Aktiveringsspenning 100 – 150 V
  - Væske ikke akseptert i IC-industrien

Kvikksølv-svitsj

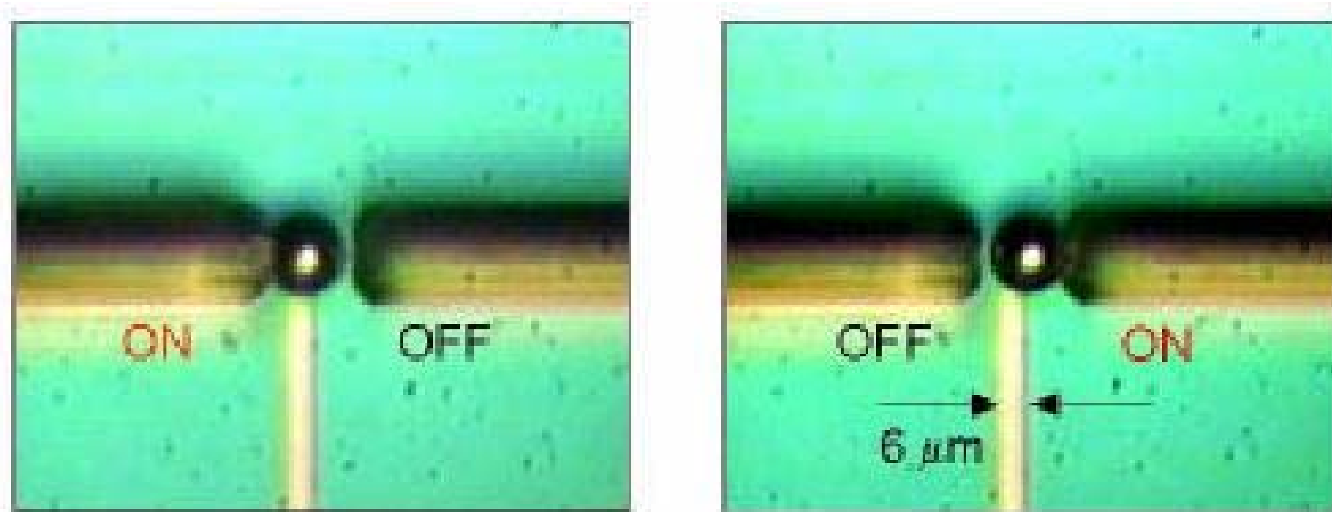

Planar prosess, foto, JHU, Appl Physics Lab

Kvikksølv-svitsj

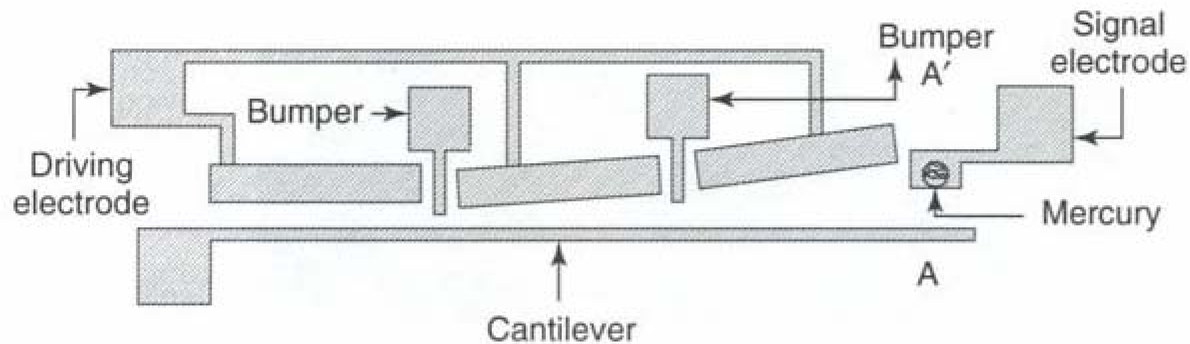

Figure 3.33 Schematic diagram of the mercury contact micro relay. Reproduced from S. Saffer, J. Simon and C.J. Kim, 1996, 'Mercury contact switching with gap-closing microcantilever', *Proceedings of SPIE*, 2882: 204–209, by permission of SPIE

Kvikksølv-svitsj

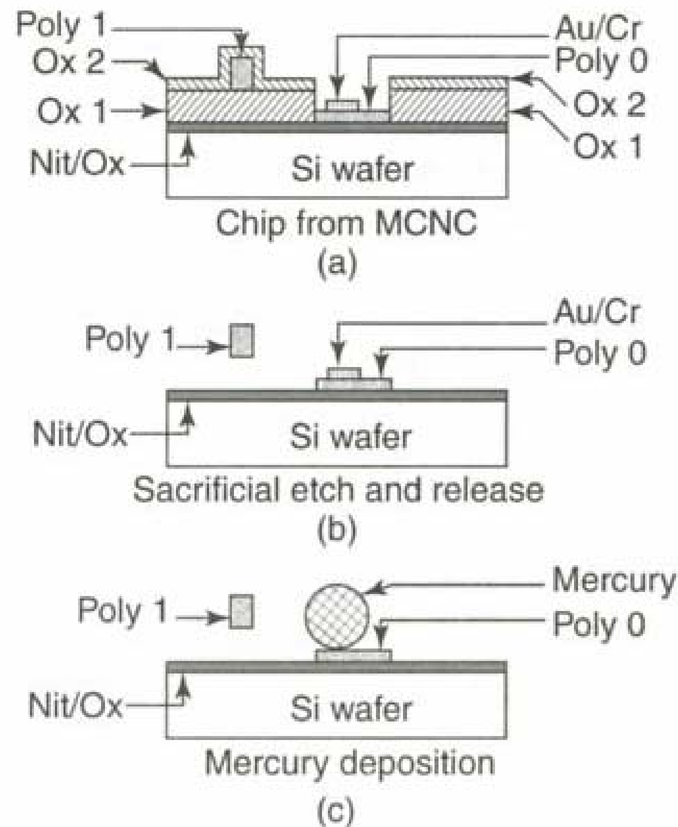

Figure 3.34 Process flow at cross-section AA′ of Figure 3.33. Note: MCNC, Microelectronics Center of North Carolina. Reproduced from S. Saffer, J. Simon and C.J. Kim, 1996, 'Mercury contact switching with gap-closing microcantilever', *Proceedings of SPIE*, 2882: 204–209, by permission of SPIE

Varadan

Termisk svitsjing

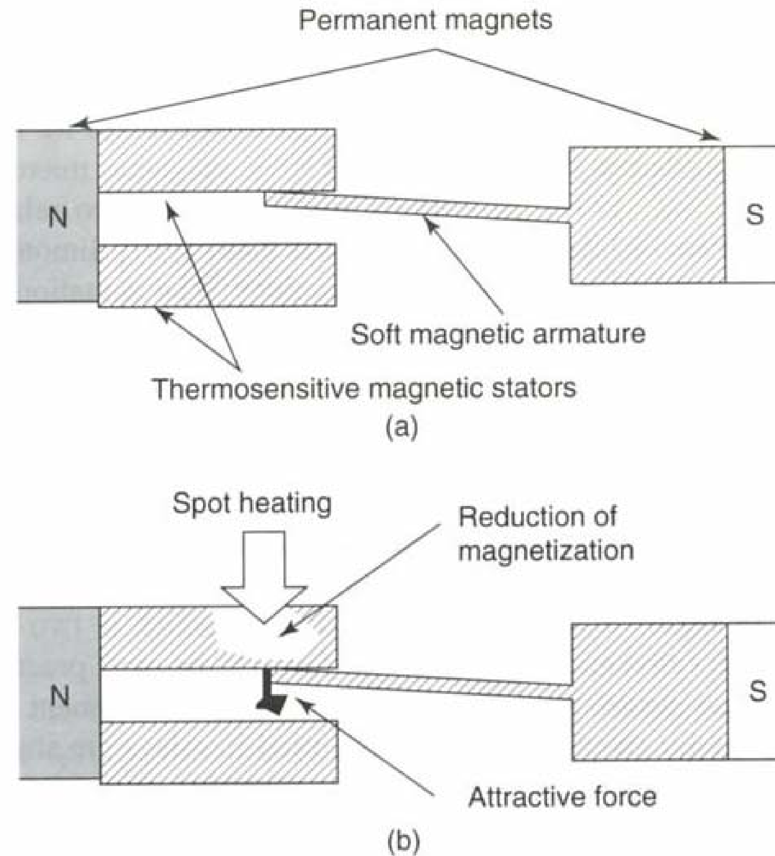

Figure 3.38 Principle of operation of thermally controlled magnetization micro relay. (a) without heat; (b) with heat. Note: N, north; S, south. Reproduced from E. Hashimoto, H. Tanaka, Y. Suzuki, Y. Uensishi and A. Watabe, 1994, 'Thermally controlled magnetic actuator (TCMA) using thermo sensitive magnetic materials', in *Proceedings of IEEE Microelectromechanical Systems Workshop, 1994*, IEEE, Piscataway, NJ, USA: 108–113, by permission of IEEE, © 1994 IEEE

Varadan

Noen utfordringer

- Høyt elektrisk felt i små dimensjoner
  – Deler av metall-overflaten kan smelte
  – Væske-metall-damp fortsetter ledningen når svitsjen er i av-tilstand
- Selvaktivering
  – Hvis signalet, som kan være lite, overlagres et DC-signal, kan det forekomme **selvaktivering**
  – Det kan derfor være en fordel å dekoble aktiverings- og signal-linjer
    - Separate områder

RF MEMS switch vs. frequency

G. Rebeiz, "Short course on RF-MEMS", Dec. 2003
H. Tilmans, Microwave week, 2004.

Equivalent circuit

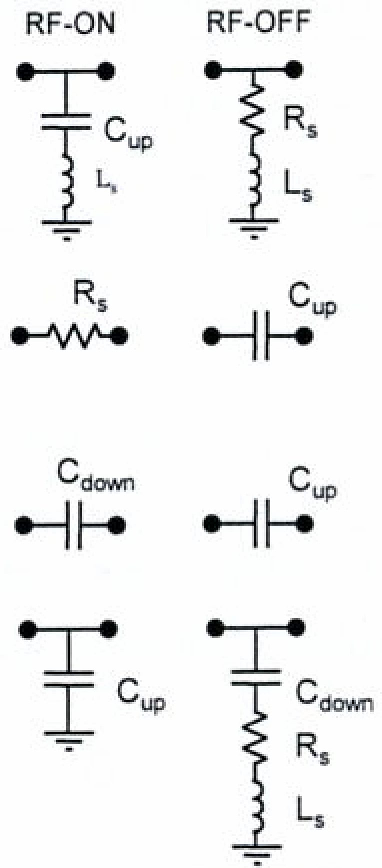

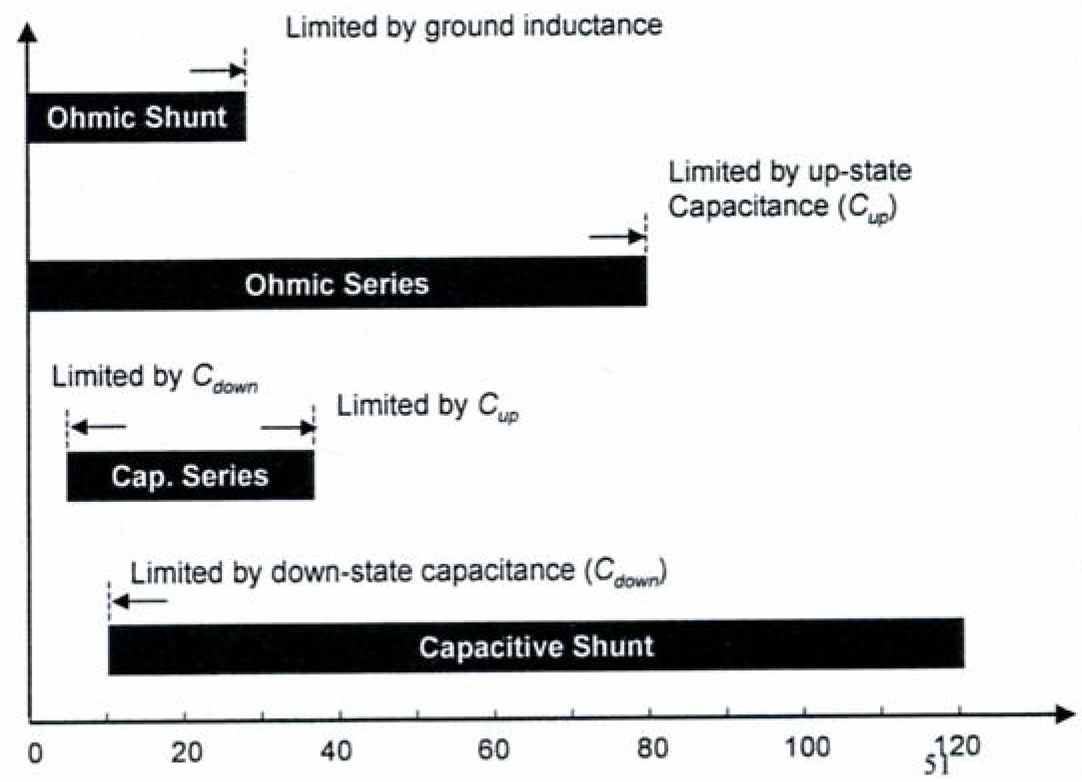

Svitsj integrert med IC

2318 IEEE JOURNAL OF SOLID-STATE CIRCUITS, VOL. 38, NO. 12, DECEMBER 2003

An Above IC MEMS RF Switch

Daniel Saias, Philippe Robert, Samuel Boret, Christophe Billard, Guillaume Bouche, Didier Belot, and Pascal Ancey

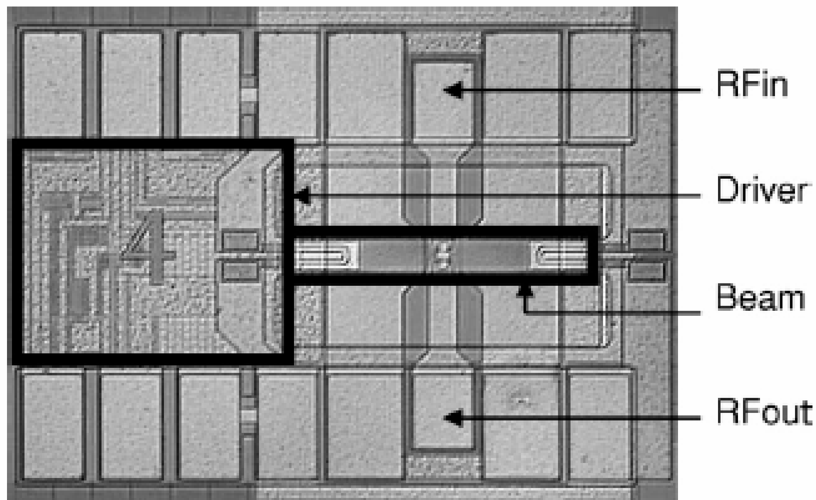

Fig. 9. Switch and driver die Micrograph.

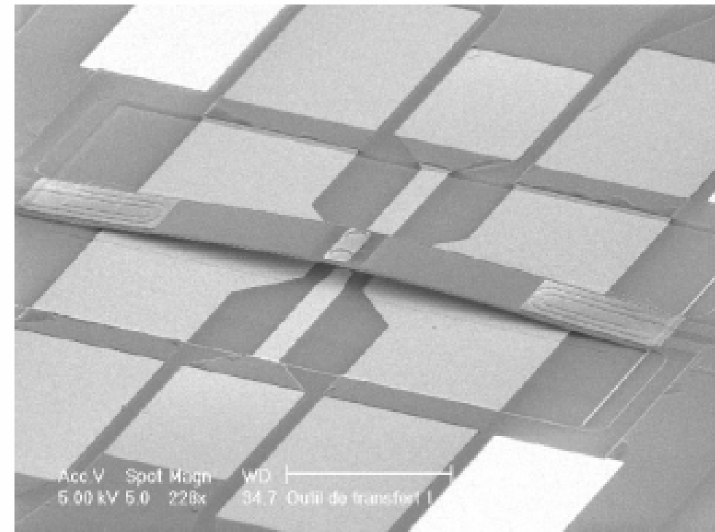

Fig. 1. SEM view of the microswitch.

Saias et al, 2003

Ytelse ved ulike løsninger

TABLE II
RF SWITCHING DEVICES COMPARED PERFORMANCE

	FET switch [2]	SOI CMOS Tx/Rx Switch High Resistivity substrate [3]	Stand alone MEMS solution [4]	Integrated MEMS (this work)
Insertion Loss	**2 @ 6GHz**	**0.7 @ 2.5GHz**	**0.15 @10GHz**	**0.4 @6GHz**
Isolation (dB)	**-20 @ 6GHz**	**-50 @ 2.5GHz**	**-15 @10GHz**	**-40 @6GHz**
Rs series (Ohm)				**2**
Cup series (fF)				**1**
Size (um x um)	**~1mm²**	**0.02mm²**	**120x280**	**300x900**
Switching time	**10ns**	**10ns**	**5.3us**	**~250us**
Actuation	**--**	**--**	**Electrostatic**	**Thermal + Electrostatic**
Driver	**--**	**--**	**External**	**Internal (300umx300um)**
Integration	**GaAs embedded**	**SOI design / Separate Chip**	**Separate chip**	**embedded**

Saias et al, 2003